Development of a Stably Aligned, Schwann Cell Seeded Composite Biomaterial that Supports Neurite Outgrowth for Neural Tissue Engineering Applications

by

Daniel G. DeWitt

A Thesis Submitted to the Graduate

Faculty of Rensselaer Polytechnic Institute

in Partial Fulfillment of the

Requirements for the degree of

MASTER OF SCIENCE

Major Subject: BIOMEDICAL ENGINEERING

Approved:

_____

Deanna M. Thompson, Thesis Adviser

Rensselaer Polytechnic Institute
Troy, New York

May, 2009

CONTENTS

LIST OF FIGURES

ACKNOWLEDGMENT

The author would like to acknowledge first and foremost Dr. Deanna Thompson and Dr. Jan Stegemann for their continued guidance and support throughout this project. Without their foresight and vision, this work could not have been accomplished.

Also, the author would like to thank Dr. Chris Bjornsson, Karen Ellison, Angela Seggio, Abigail Eldridge, and Megan Farrell for their technical assistance. This work was supported by the New York State Spinal Cord Injury Research Program IDEA #J50480 (DMT and JPS) and completed in the Center for Biotechnology and Interdisciplinary Studies (CBIS) at Rensselaer.

ABSTRACT

Spinal cord injury (SCI) is a devastating condition due to trauma, sports-related injuries and disease resulting in varying degrees of paralysis, reducing a patient's quality of life and lowering life expectancy. Despite the capacity for regeneration, there is no functional treatment for SCI due to the hostile microenvironment of the spinal cord following injury. A host of variables inhibit nerve regeneration such as glial scarring, cell death, removal of myelin, lack of a permissive substrate and an inadequate level of growth factors. Due to the complexity, there is likely not one single therapeutic intervention that will solely control regeneration. Rather, the synergistic combination of various guidance cues (e.g. soluble factors, substrate composition, cellular, chemical, electrical, mechanical, or topographical) will be necessary to promote nerve regeneration and develop a clinically effective therapy for SCI.

Investigation of various guidance cues in a 3D model is necessary to carefully investigate neuronal and glia response prior to *in vivo* experimentation. The goal of this thesis is to present the development and characterization of a novel, stably aligned composite biomaterial to serve as a platform to investigate guidance cues on neurite outgrowth. One aim of this work was to develop a biomaterial concurrently supportive of both Schwann cells (SC) and neurons. This was accomplished by combining collagen I and Matrigel™ at a 65/35 volume/volume ratio. SC viability was consistently high and cells were able to spread in this composite biomaterial. Also, this composite biomaterial is supportive of both neurite outgrowth and Schwann cell migration. A second aim was to stably align the cellular and matrix components of these scaffolding materials. Alignment is useful in directing neurite outgrowth and was accomplished through the use of fibroblast (FB) mediated compaction. Following the removal of constraint, stable alignment of SC, FB, and collagen I was observed for at least 7 days in culture. Finally, neurite outgrowth within these constructs was examined and aligned matrices have the ability to direct this outgrowth in 3D space.

Future studies will involve combining guidance cues such as soluble factors or electrical stimulation with these aligned and unaligned SC loaded collagen I-Matrigel™ biomaterials. Relative strengths of each cue, as well as synergistic effects, may be examined to aid in the development of a therapeutically viable SCI implant.

1. Introduction and Historical Review

1.1 Spinal Cord Injury at a Glance

Spinal cord injury (SCI) is a debilitating condition affecting over 250,000 Americans alone, with an estimated 12,000 new cases occurring each year, according to the National Spinal Cord Injury Statistical Center.[1] Aside from the high costs, which can eclipse $3 million lifetime for a high tetraplegia patient, sufferers of SCI experience a marked decrease in quality of life. Depending on the location of the injury within the spinal cord, symptoms can range from loss of bowel function to paralysis of the legs (paraplegia) for low SCI injuries, loss of the ability to breathe without a ventilator (tetraplegia), and death in high SCI injuries. In all cases, the life expectancy of these patients is substantially decreased and additional risks such as blood clots and ulcers caused by a lack of movement complicate this condition further. Presently, a therapeutic cure for SCI does not exist, creating a void for the biomedical sciences to fill so that these patients may regain lost functions from an injury.

Reasons why regeneration does not occur in the spinal cord following injury are numerous, making this an especially difficult condition to treat. Studies have demonstrated that CNS neurons, once thought to be void of the ability to regenerate, are actually able to regrow short distances at the lesion site and sprouting from surviving axons has been reported in some cases.[2, 3] In fact, when peripheral nervous system (PNS) tissue is implanted at CNS lesion sites, CNS axons have shown to penetrate the PNS tissue and growth only stalls when native CNS tissue is again reached.[4] Studies such as these have pointed towards the inhibitory microenvironment resulting from trauma and not an intrinsic inability of CNS axons to regenerate as the major obstacle to overcome in nerve repair strategies.

Within the inhibitory lesion microenvironment there are a number of components at play which prevent the proper regrowth of CNS axons. The formation of a glial scar by astrocytes, a CNS specific glial cell, has gained much attention as one of the primary causes for regeneration failure. Preliminarily, it was believed that this glial scar simply formed a physical barrier, preventing axonal extension through the glial scar and effective reinnervation of proximal axons to the distal nerve stump.[5] It has become

increasingly apparent, however, that the production of inhibitory molecules plays an important role in regeneration failure as well.[6-8] Proteoglycans (e.g. chondroitin sulphate proteoglycans), myelin-associated inhibitory molecules (e.g. myelin associated glycoprotein (MAG) and P0), and a host of other molecules have all shown to be both present at the injury site and inhibit axonal outgrowth *in vitro* and *in vivo*.[6, 9-15] Davies et al (1999) examined the response of dorsal root ganglia (DRG), sensory neurons of the peripheral nervous system, when microscopically implanted into intact or lesioned spinal cords. Within the intact microenvironment, sensory axons (DRG) extended long distances through the spinal tract. However, when these growing axons encountered a lesioned area, growth cones adopted a dystrophic state and axonal penetration halted, clearly pointing towards the inhibitory microenvironment as a primary cause of CNS regeneration failure.[16, 17]

1.2 CNS Nerve Repair Strategies

In an effort to overcome this inhibitory microenvironment, a number of different approaches have been taken with two basic trains of thought: 1) promoting axonal regeneration and 2) modifying the local microenvironment. Although CNS neurons do possess the ability to regenerate, their regeneration potential is seen to be less than that of peripheral neurons.[17] Therefore, if axon regeneration can be enhanced following injury there stands a better chance that successful reconnection of the injured spinal cord will occur. As opposed to directly trying to activate axon outgrowth, these approaches involve altering the lesioned area to make it more permissive of regeneration. Outlined below is an array of experimental approaches which follow these two trains of thought.

Enhancing the intrinsic ability of neurons to regenerate is typically done in one of two ways: through the addition of soluble neurotrophic factors or by altering gene expression so that growth-promoting genes are overexpressed.[18] Recent studies have indicated that the neuronal genes GAP-43, c-jun, and Bcl-2 play important roles in nerve regeneration. Interestingly, these genes are expressed differently in variable neuronal populations, and neurons which have a higher intrinsic ability to regenerate, such as PNS neurons, constitutively express these genes at a higher level.[19, 20] It is hypothesized that

by controlling expression of these genes, the overall growth potential of CNS neurons may be enhanced to promote regeneration.

Application of neurotrophic factors offers another avenue for enhancing the regeneration potential of CNS neurons. Nerve growth factor (NGF) has shown promise in the treatment of SCI in animal models.[21] One study transplanted fibroblasts (FB) genetically modified to secrete NGF within a spinal cord lesion and extensive growth of sensory axons into the graft material was observed. Motor neurons and corticospinal neurons, however, failed to respond in an equally robust manner, no axons left the graft material or re-entered the host spinal cord, and functional recovery was not substantially improved after a year.[22, 23] This work confirmed NGF as a specific stimulus for sensory axons. Alternatively, brain-derived neurotrophic factor (BDNF) has been demonstrated to be an attractor of both motor and sensory axons.[24, 25] Following spinal cord transection rats given a continuous infusion of BDNF for 28 days following injury exhibited slight improvements in locomotion scores relative to untreated controls. Rats treated with BDNF regained the ability to air-step with their hind legs, however a full functional recovery was not achieved.[24]

Glial cell-line derived neurotrophic factor (GDNF) and neurotrophin-3 (NT-3), both neurotrophic factors, have demonstrated utility in treating SCI. Similar to BDNF, GDNF has a demonstrated ability to enhance both sensory and motor axon penetration into a graft material in comparison to untreated controls. Corticospinal axonal growth, which is necessary for full functional recovery, was not enhanced by GDNF application in rats.[26] However, NT-3 is the only growth factor to date with a demonstrated ability to promote corticospinal axonal regeneration. In one study, a single injection of NT-3 at the lesion site resulted in substantial sprouting of corticospinal axons which was not seen with an equally dosed injection of BDNF.[27] Subsequent studies transplanted FB genetically modified to constitutively express NT-3 at the spinal cord transection site and over the course of 3 months substantial, although not full, functional recovery of rats was observed. Similar recovery was not observed in untreated control groups.[28] Collectively, these studies specifically highlight potential applications for the delivery of different neurotrophic factors. Although no one factor appears to be a cure-all, and these studies serve to gain a better understanding of how neurotrophic factors interact with

regenerating axons as a vehicle to support axonal regeneration for a therapeutic treatment for SCI.

Moving away from specifically promoting axonal outgrowth, a substantial body of work has also been devoted to modifying the inhibitory microenvironment. These approaches fall into one of four categories: implantation of acellular grafting materials, cellular transplantation, clearance of inhibitory debris from the lesion site, and permeabilization of the glial scar. Each of these will be discussed briefly as will the potential benefits of combining treatment strategies.

Grafting materials have been used for decades in nerve treatment strategies and although many different types have demonstrated utility, none have resulted in full functional recovery to date. The main idea behind the grafting approach is that the implanted material will create a more favorable environment for axons to penetrate than the existing CNS lesion site. Aside from supporting outgrowth, these grafts must also provide some directional cue to guide the regenerating axons to the target distal nerve stump. Artery, vein, and muscle grafts have a long-standing history of enhancing regeneration in both the PNS and CNS.[29-34] Graft materials provide a natural tubular guidance channel for analysis. More recently, acellular allogenic nerve grafts have attained regeneration comparable to that seen when nerve autografts, the current gold standard, are used.[35] Previous studies have attempted to use degradable biomaterials to provide an initial guidance channel which will disappear over time, to be replaced by new CNS tissue. For instance, one group implanted only aligned collagen I fibrils into a 5 mm spinal cord defect in rats and after 12 weeks, an increase in functional recovery and greater numbers of axons were found traversing the graft when compared to controls. However, nearly 50% of the collagen had been degraded by this time point.[36, 37] Alginate, a polysaccharide derived from algae, has been used to demonstrate the utility in both promoting axonal regeneration across a CNS lesion and in reducing the number of reactive astrocytes thereby limiting the negative effects of the glial scar.[38, 39] Other degradable scaffolds which have shown promise in promoting CNS regeneration include, but are not limited to, hyaluronic acid, chitosan, PLGA, PLLA, polycarbonate, and polyethylene glycol.[40-43] Non-degradable scaffolding materials such as poly(2-hydroxyethyl methacrylate) (PHEMA) have the added benefit of structural stability over

their degradable counterparts and their use has also demonstrated utility in SCI repair.[44] The continued presence of a graft material at the injury site presents additional challenges such as long-term biocompatibility. Despite the beneficial aspects of each of these different scaffolding materials, a full, functional recovery was not achieved by the aforementioned grafts. From just this abbreviated list, it is easy to see that the range of materials which may be used for SCI repair is immense. It is the job of researchers to gain a better understanding of exactly how regenerating axons respond to each material and what are the key features which need to be incorporated so that a scaffold may be optimized.

Cell transplantation is another approach which has gained considerable attention and also attained promising, yet incomplete, results. Schwann cells, glia from the PNS, have been implanted in CNS nerve injuries and support axonal extension. This approach will be covered in more depth in next section of this work, as it is one of the focal points of my master's thesis, but as early as 1911, it was realized that PNS tissue, specifically Schwann cells, significantly enhanced CNS axonal regeneration.[45] Transplantation of autologous CNS glial cells, such as astrocytes or olfactory ensheathing glia (OEG) have proved beneficial in promoting functional recovery following SCI. One benefit of this approach is that is does not introduce foreign cells to the injury site thereby circumventing possible complications associated with this additional variable. Implantation of astrocyte progenitor cells, which are known to release high levels of neurotrophic factors, aided in preventing glial scar formation in a rat SCI model.[46, 47] OEG transplantation is desirable because, aside from promoting axonal regeneration, there is some evidence that these cells are able to myelinate axons if properly stimulated.[48] More recently, considerable attention has been given to the implantation of neural progenitor cells (NSC) at the injury site. These cells have the distinct advantage of not being fully differentiated and, as such, are capable of forming neurons and glial cells alike. This offers the possibility of transplanting only stem cells and promoting differentiation of both glial cells and neurons. NSC administered to an SCI defect in mice resulted in significant locomotor recovery and myelination of regenerating axons was observed.[49] These effects were abolished if NSC were not implanted.[49] Knowledge of NSC differentiation remains incomplete limiting the current therapeutic application of

this approach. Other cells types commonly implanted include olfactory ensheathing glia and microglial cells.[18] As with the grafting materials, each cell type garners a specific, typically beneficial, response in the injured spinal cord, yet the effects of one individual component remain inadequate for recovery.

The injury microenvironment may also be modified via the removal of inhibitory molecules. Vaccine immunization against myelin or myelin components, which are known to be inhibitory of regeneration, enhances regrowth of the corticospinal tract.[50, 51] Additionally, antibodies against the proteins Nogo-A, Nogo-C, and myelin-associated glycoprotein, identified as inhibitory proteins, increase the ability of corticospinal neurons to reestablish severed connections created during injury by making the microenvironment less inhibitory.[52, 53] The amount of work which has been devoted to the neutralization of repulsive cues following injury is immense and much of it resides beyond the scope of this paper. Given their repulsive nature, elimination of these cues will likely be a component of a final therapeutic combinatorial approach.

A final avenue for modifying the microenvironment following injury involves permeabilizing or reducing the formation of the glial scar. As mentioned, the production of proteoglycans by reactive astrocytes in the scar is a major obstruction in the successful regeneration of neurons across a spinal cord lesion. Enzymatic degradation of these proteoglycans, specifically choindroitinase sulphate proteoglycan, has shown to increase sprouting of neurons following SCI thereby promoting regeneration.[54-56] Other attempts have used enzymes such as collagenase or trypsin to try to permeabilize and degrade the glial scar but these were met with only limited success, as it has become more apparent since that the molecular composition of the scar is more inhibitory than the physical barrier of the glial scar.[57, 58] Still, reduction of the glial scar and the inhibitory molecules will be beneficial to axonal extension although this reduction alone is unlikely to result in full functional recovery.

As evidenced by the array of complicating variables present at spinal cord lesions which prevent regeneration and the plethora of approaches employed to overcome these variables, it should be clear that SCI is a complex, challenging injury to fix. All the above attempts, and many others, have provided valuable information regarding CNS axonal regeneration but, ultimately, all these attempts have come up short of achieving

full functional recovery. What has become apparent is that successful treatment will likely employ a combinatorial approach of a number of the experiments outlined above. Combinatorial approaches have been vigorously investigated in recent years and some promising results have been attained using these methods. In one set of studies, SC filled guidance channels implanted into transected rat spinal cords resulted in significantly more axon re-growth when compared to controls without embedded SC or without a guidance channel[59, 60] and entry into the distal nerve stump was reported in hemisected spinal cords when SC loaded mini-channels were used.[61] In another work, NSC loaded in a PLGA scaffold and implanted into a mouse SCI model resulted in functional recovery, consisting of coordinated weight bearing hind-limb stepping after 70 days. This recovery was not observed if the scaffold or cells were missing from implantation.[62] Combinatorial therapies of peripheral nerve grafts or Schwann cell loaded grafts combined with the neurotrophic factors NT-3, BDNF, or fibroblast growth factor improved functional recovery compared to each therapy alone demonstrating the potential synergistic effects which may be achieved by combining different approaches.[63, 64]

Despite the incremental successes, a cure for SCI remains elusive. It is important to understand how different guidance cues interact so that so that a refined and optimized combinatorial approach may be applied to treat SCI. **This thesis is focused on developing a scaffold that is supportive of Schwann cell migration and neurite outgrowth. Specifically we developed a novel, Schwann cell loaded biomaterial comprised of collagen I and Matrigel™ with an aligned cellular component for studying the effects on 3D neurite outgrowth. Below is relevant background pertaining to the specific components of the scaffolding materials.**

1.3 Schwann Cell (SC) Functions

Due to their close relationship with neurons, SC have been widely used in nerve repair strategies. SC are the glial support cells of the PNS and all neurons in the PNS are in contact with one or more SC, which are responsible for myelination of individual axons.[65] SC are also responsible for the concentration of ion channels at the nodes of Ranvier and therefore contribute to the rapid conduction of action potentials.[66, 67] In

addition, both during development and following injury, SC provide a number of trophic factors to growing axons[68] and they produce proteins such as collagen type IV[69] and laminin[70] that form the extracellular matrix of the nervous system. Importantly, SC have been closely linked to nerve regeneration. Following injury and Wallerian degeneration in the PNS, SC can remove myelin and proliferate extensively to form bands of Bunger, creating a cable between the proximal and distal nerve stumps;[71] this rapid SC proliferation is a key event in promoting axonal re-growth lending insight that SC play a pivotal role in the ability of the PNS to regenerate.[72] Due to these properties, SC have been used extensively in nerve repair strategies both in the PNS and CNS.

1.4 Schwann Cells and Peripheral Nerve Regeneration

These properties have made SC of interest for the guidance of neurites and PNS nerve regeneration both *in vitro* and *in vivo*. Guidance of growing axons is a necessary component of any nerve repair strategy as it is imperative that these axons reconnect with their proper target. In culture, it has been demonstrated that a SC substrate enhances neurite outgrowth when compared to non-glial cells[73] and oriented SC are able to promote neurite alignment and growth on micropatterned PLLA substrates with localized laminin patterns.[74] Subsequent work has shown that oriented SC alone were able to direct neurite outgrowth, in the absence of any other guidance cues.[75] *In vivo*, Guenard, et al. demonstrated neurite outgrowth in rat sciatic nerves following injury using Matrigel™ filled semi-permeable guidance channels seeded with SC. This work also provided evidence that SC seeding density correlated to the amount of neurite extension into the grafts.[76] Using a similar approach poly(L-lactide-co-e-caprolactone) guides were filled with SC loaded Matrigel™ and used for the repair of 6 mm sciatic nerve defects in mice. Functional recovery in this model approached that observed using autologous nerve grafts, emphasizing the importance of SC in peripheral nerve regeneration.[77]

1.5 Schwann Cells for Spinal Cord Repair

Although SC are PNS glia, they have demonstrated utility for treating injuries of the central nervous system (CNS).[60, 78, 79] Following traumatic injury, some SC will migrate

into the CNS where they can play a role in endogenous repair processes.[80] However, SC and CNS glia (astrocytes) do not typically intermingle and SC rarely leave the graft material when implanted in CNS grafts. *In vitro*, SC have shown to have properties which promote CNS neurite outgrowth and Noble, et al. (1984) showed that this outgrowth was comparable to that seen on astrocyte substrata.[81] Modest growth and functional recovery have been reported in rats after the transplantation of human SC at the injury site following spinal cord transection[79] and remyelination of CNS axons by autologous SC has also been demonstrated in monkey models.[78] One study highlighted that the transplantation of SC in a 5 mm spinal cord defect resulted in more axon outgrowth into the graft and greater functional recovery than a comparable transplantation of olfactory ensheathing glia, which are native glia of the CNS.[82] Collectively these studies suggest that SC play an important role in nerve regeneration not only in the PNS but in the CNS as well. For these reasons, we sought to incorporate SC as a central component of the scaffolding material.

1.6 Collagen I and Matrigel™: Biomaterials for CNS Nerve Repair

As evidenced in the section regarding nerve grafts, a wide array of materials have been used in approaches to repair SCI, with variable levels of success. Two materials commonly used in nerve repair strategies are collagen I and Matrigel™, as they each have desirable properties for neural engineering applications. Collagen I is one of the most abundant proteins in the human body, accounting for approximately 30% of the total amount of protein.[40] In addition, collagen I is found in close proximity to axons, as it comprises part of the endoneurium which surrounds the Schwann cell-axon units in the PNS.[83] Collagen I hydrogel is a relatively mechanically robust, fibrillar protein and has the unique advantage that the fibrils can be directionally aligned. Alignment is desirable for the guidance of axons through a scaffold and since collagen I is known to be supportive of neurite outgrowth, it has been commonly used in guidance channel studies.[36, 77, 84, 85]

Despite these advantages, a recent study highlighted that, although collagen I is supportive of axonal outgrowth, it may not, in itself, be a suitable material for supporting glial cells, specifically SC.[86] In work by Rosner, et al., (2005) it was reported that SC

embedded in 3-D collagen I gels exhibited a spherical morphology, indicative of little interaction with the matrix material. Cellular extension is necessary for SC survival and, typically, cultured SC exhibit a bipolar, extended morphology. Numerous modifications were made to the collagen I scaffolds in this study in an effort to elicit a spread morphology from the SC. Collagen I concentration in the gel was varied, soluble laminin was added at concentrations up to 100 μg/ml, and a number of growth factors, including TGF-β1, were incorporated. Of these attempts, only the addition of TGF-β1 (at 0.5, 2, or 20 ng/ml) resulted in a significant increase in cell spreading; over 50% of SC in all cases were in an extended morphology after 10 days in culture compared to less than 10% without TGF-β1. Even still, cellular protrusions were small and 50% of the cells remained unspread. If aligned SC are to be used to guide neurite outgrowth, cellular processes on the SC are a necessity.[86]

To create a biomaterial scaffold that was both supportive of neurite outgrowth and Schwann cell spreading, we sought to modify collagen I matrices by the addition of Matrigel™. Matrigel™ is a mixture of basement membrane proteins developed in mouse Engelbreth-Holmes-Swarth tumor cells and is comprised of approximately 60% laminin, 30% collagen IV, and 7% entactin.[87] Laminin and collagen IV are two prominent, endogenous basal lamina proteins in direct contact with SC-axon units in peripheral nerves.[83] The hypothesis was that the addition of components in the natural basal lamina would support SC spreading. Matrigel™, however, has the distinct drawback of being mechanically brittle. As such, it is difficult to handle, without damaging and does not contain robust fibers for alignment. Collagen I satisfied these needs, and the composite matrix is used as a model material for these studies.

Previous work in this field has focused on the optimization of scaffolding environments solely for neurons. Although neurons and axonal re-growth are clearly vital for functional nerve regeneration, complete recovery may not be achieved if the glial population is overlooked. Glia support axonal outgrowth by the production of soluble factors and the production of ECM, but SC also myelinate the regenerated axon. Schwann cell migration and spreading in novel biomaterials is less well studied. Due to the number of beneficial processes which SC performs, it is likely that the creation of a scaffold material that is optimized for SC support as well as for neurons will yield

improved results. The development of a biomaterial concurrently supportive of SC and neurons, yet still mechanically robust, is the first specific aim of this work.

1.7 Scaffold Alignment

It has been well documented that scaffold and/or cell alignment promote the directed outgrowth of neurites both *in vitro* and *in vivo*.[84, 85, 88, 89] Neurons respond to physical guidance[90, 91] and the creation of an oriented scaffolding material to direct axonal growth in conjunction with cellular cues, such as aligned SC, could increase the probability and rate that axons successfully traverse a spinal cord lesion. For this reason, the development of an aligned scaffold, both supporting SC migration and spreading, was a goal of this work.

Previous work has portrayed the utility of aligned collagen I scaffolds in neural engineering. In a 6 mm rat sciatic nerve defect, collagen only guidance channels aligned using a strong magnetic field promoted some functional recovery in 100% of tested rats compared to 17% for untreated controls. [84] This system, however, was not investigated in the CNS and it is not known whether collagen fibrils remained aligned over an extended period in culture without the magnetic field.[84] In the CNS, aligned collagen I filaments created from enzymatically digested skin were implanted into a 5 mm rat spinal cord defect and garnered some functional recovery. After 12 weeks, rats were able to walk and climb, and axons could be seen entering the proximal end of the graft and exiting the distal end where they were then observed reentering the host spinal cord. [36] There was not, however, any combinatorial component to this graft.

Oriented scaffolds can be created by constrained compaction. FB are known to compact collagen I matrices and if compaction is constrained in one dimension, cells will align in the direction of compaction.[92] Although this approach did show promising results in PNS nerve regeneration, constructs were not assessed for alignment after removal of constraint.[93] Additionally, constraint introduces the variable of tension to the system which complicates understanding which components are specifically affecting neurite outgrowth. For this work, we hope to use FB mediated constrained compaction to orient the Schwann cells and scaffold. This approach does not require the use of any specialized equipment, FB are native cells of the nervous system, and FB will

spontaneously compact and align collagen I with no external stimulation. Based on this, a second specific aim of this work was to create stable, aligned SC loaded collagen I-Matrigel™ scaffolds using cell mediated compaction without the continued presence of an external constraint apparatus.

1.8 Neurite Guidance

After reading this introduction it should be clear that there are a host of factors at play in dictating nerve regeneration and therefore a number of places for interjection in attempts to promote recovery. Axon guidance across an injury site is of vital importance in achieving functional recovery for these axons must reconnect with their proper target. It has been demonstrated that the guidance of axons can be accomplished in a number of ways as axons respond to a variety of cues. These cues include soluble chemical cues[21, 94, 95], physical cues[74, 90], cellular cues[75, 81], substrate specific cues[88, 96, 97], mechanical cues[98], and electrical cues.[99, 100] Although it has been well established that neurons do, indeed, respond to these cues, what is not known is the specific contribution of each cue to neurite outgrowth and the possible synergistic effects which may be achieved by combining cues in 3D microenvironments.

1.9 Project Overview

Spinal cord injury is a complex injury with an array of obstacles which must be overcome for full functional recovery to be achieved. It has become apparent that a combinatorial therapeutic approach will likely be necessary to achieve this level of recovery and, as such, it is important to study the individual and synergistic effects of multiple guidance cues on neurite outgrowth. The ultimate goal of this work was to develop a novel aligned, SC loaded, collagen I-Matrigel™ scaffold for neural engineering applications. In doing so, the effects which each graft component- aligned cells and aligned matrix- has on *in vitro* neurite outgrowth could be examined. Gaining a better understanding of how these guidance cues affect 3D neurite outgrowth will allow for the more efficient development of a therapeutic SCI treatment so that an effective combinatorial treatment, containing a range of the components described throughout this introduction, can be realized.

To this end, this work has three specific aims:

1. Create and characterize a relatively mechanically robust scaffolding material comprised of collagen I and Matrigel™ which will be concurrently supportive of Schwann cells and neurons.
2. Create stably aligned matrices containing SC using cell-mediated constrained compaction.
3. Examine the effects of aligned cells, aligned matrices, and both on 3D neurite outgrowth through the scaffolding materials.

The work presented within this thesis describes the creation of a scaffolding material which will serve as a platform for investigating the synergistic effects of multiple cues on neurite outgrowth. A composite biomaterial comprised of collagen I and Matrigel™ was used as model material as it is concurrently supportive of neurons and Schwann cells. Subsequently, a method for creating stable, aligned versions of this scaffold is also described. This method results serves to align both the matrix component and glial component in 3D scaffolds. Concurrently, these biomaterials are supportive of SC spreading and migration as well as neurite outgrowth and pilot studies show that these scaffolds can direct outgrowth within the composite biomaterial. Subsequent studies may use this biomaterial to investigate the relative strength of guidance cues *in vivo*. In the future, a number of the other cues discussed, specifically soluble and electrical cues, may be applied to examine synergistic effects on both SC migration and neurite outgrowth. Ultimately, this field is working toward the development of a novel scaffold to create a therapeutically relevant scaffold for SCI.

2. Chapter 2: Collagen I-Matrigel™ Scaffolds for Enhanced Schwann Cell Survival and Control of 3D Cell Morphology

*This chapter has been published in Tissue Engineering. The full citation is:

Dewitt DG, Kaszuba SN, Thompson DM, Stegemann JP. Collagen I-Matrigel scaffolds for enhanced Schwann cell survival and control of 3D cell morphology. Tissue Eng Part A. 2009 Feb 20. [E-published ahead of press]

2.1 Abstract

We report on the ability to control 3-D Schwann cell (SC) morphology using collagen I-Matrigel™ composite scaffolds for neural engineering applications. SC are supportive of nerve regeneration following injury and it has recently been reported that SC embedded in collagen I, a material frequently used in guidance channel studies, do not readily extend processes, instead adopting a spherical morphology indicative of little interaction with the matrix. We have modified collagen I matrices by the addition of Matrigel™ to make them more supportive of SC and characterized these matrices and SC morphology in vitro. Incorporation of 10%, 20%, 35%, and 50% Matrigel by volume resulted in 2.4, 3.5, 3.7, and 4.2-fold increases in average SC process length after 14 days in culture compared to collagen I only controls. Additionally, only 35% and 50% Matrigel™ constructs were able to maintain SC number over 14 days while an 86% decrease in cells from the initial seeding density was observed in collagen only constructs over the same time period. Mechanical testing revealed that the addition of 50% Matrigel™ increased matrix stiffness from 6.4 kPa in collagen I only constructs to 9.8 kPa. Furthermore, second harmonic generation imaging showed that the addition of Matrigel™ resulted in non-uniform distribution of collagen I and scanning electron microscope imaging illustrated distinct differences in the fibrillar structure of the different constructs. Collectively, this work lays a foundation for developing scaffolding materials which are concurrently supportive of neurons and SC for future neural engineering applications.

2.2 Introduction

Current treatments for patients suffering from spinal cord injury (SCI) rarely result in full functional recovery, necessitating the development of new therapeutic approaches. Schwann cells (SC) are currently being investigated as a component of nerve repair

strategies in the central nervous system (CNS) due to their close relationship with neurons in the peripheral nervous system (PNS).[65, 66, 68-70] SC play an important role in the PNS and a number of studies have demonstrated the beneficial effect SC have on nerve regeneration.[71, 72, 74-77]

For these reasons, SC have been used in CNS nerve repair strategies with promising results despite being resident cells of the PNS. In vitro, CNS neurite outgrowth can be supported by both SC and astrocyte substrata.[81] In vivo, SC filled guidance channels implanted into transected rat spinal cords resulted in significantly more axon extension when compared to acellular controls.[59, 60] Entry into the distal nerve stump was reported in hemisected spinal cords when SC loaded mini-channels were used.[61] In some rare cases following injury, SC will migrate into the CNS where they can play a role in endogenous repair processes.[80] In addition to promoting axonal outgrowth, autologous SC can remyelinate CNS axons which is necessary to restore function.[78] Despite these successes, treatments for patients suffering from spinal cord injury remain inadequate and full functional recovery has yet to be achieved. Incorporation of autologous SC is a promising avenue to improve the outcome of these approaches.

Most efforts have focused on optimizing scaffolding environments solely for axonal extension, while concurrent optimization for SC remains less studied. Creation of a scaffold optimized for SC and neurons may likely yield improved results. Hurtado, et al. reported that few SC implanted in fibrin filled rat thoracic spinal cord grafts remained after 6 weeks, pointing out that SC survival needs to be improved to increase graft efficacy.[101] Additionally, Rosner, et al. recently reported that SC embedded in 3D collagen I, a material supportive of neurite outgrowth which is commonly used as a scaffold in guidance channel studies, exhibited a spherical morphology indicative of little interaction with the matrix material.[86] Although some studies have demonstrated beneficial regenerative effects using SC loaded collagen I hydrogels, none have looked specifically at SC interaction with the matrix in the absence of complicating variables such as neurons, fibroblasts, proteins, or growth factors.[68, 85, 93, 102]

It is likely that multiple cues presented in the 3D scaffold– including glia, soluble factors, scaffold geometry and composition, and external forces– act synergistically to enhance neurite outgrowth. To systematically test these variables, a scaffolding material

that is both independently and concurrently supportive of SC and neurons must be developed. Collagen I alone does not accomplish this goal, but is a promising scaffold material because it is robust enough to be easily handled and can be directionally aligned.[84, 85] We therefore have augmented a collagen I matrix with Matrigel™, a commercially available preparation of basement membrane proteins comprised of approximately 60% laminin, 30% collagen IV, and 7% entactin.[87] Matrigel™ was chosen because laminin and collagen IV are two prominent, endogenous basal lamina proteins of the nervous system that are in direct contact with SC.[83]

Our goal in this work was to develop a scaffold material that is supportive of SC spreading to serve as a platform for investigating the synergistic contributions of multiple guidance cues on neurite outgrowth. We hypothesized that the addition of Matrigel™ to collagen I would support SC spreading – defined as the appearance of protrusions from the SC and a spindle-shaped morphology – and increased SC number due to changes in the chemistry and architecture of the scaffold. We used growth factor reduced (GFR) Matrigel™ to minimize the potential effects of soluble factors. Notably, levels of IGF-1 and TGF-β1 are not effectively reduced in the GFR formulation, and therefore we controlled for this by incorporating these proteins into pure collagen I matrices. In the present study, we have characterized collagen I-Matrigel™ composite scaffolds as well as the effects of these materials on SC viability, number, and morphology. Scaffolds that are supportive of both SC and neurons will allow us to systematically investigate multiple guidance cues with the ultimate aim of developing improved SCI implants.

2.3 Materials and Methods

2.3.1 Cell Culture

Primary Schwann cells (SC) were isolated from the sciatic nerves of neonatal rats and provided as a gift from Dr. J. Salzer (NYU). Subsequent expansion of Schwann cell cultures was carried out in Dulbecco's Modified Eagle's Medium containing 4 mM L-glutamine, 4.5 g/L D-glucose, 110 mg/L sodium pyruvate (DMEM; CellGro, Manassas, VA) and supplemented with 10% fetal bovine serum (FBS; HyClone, Logan, UT), 50 U penicillin/streptomycin (Cellgro), 10 μg/ml bovine pituitary extract (BPE; Becton,

Dickinson and Company, Franklin Lakes, NJ), and 10 μM forskolin (Sigma-Aldrich, St. Louis, MO). Cells were grown at 37°C and 7% CO_2 with the media being changed every other day.[103] Cells were passaged at ~90% confluence using a 0.05% trypsin/0.53 mM EDTA solution (CellGro) and cells between passages 10-15 were used for all experiments. Prior to use, SC purity was assessed in monolayer culture using S100 staining and quantified using ImageJ (NIH). Purity levels of >95% were observed for all cultures from passages 10 to 15.

2.3.2 Construct Preparation

Following trypsinization, SC were diluted in growth medium and pelleted. SC were then resuspended in 10 ml phenol-red free growth media (CellGro) to reduce background fluorescence;[104] aside from the absence of phenol red, this growth media was identical to that described above. Cells were subsequently counted, partitioned, and pelleted again prior to use.

Each 0.5 ml construct was seeded with 500,000 cells in 24 well plates (BD Biosciences, San Jose, CA) resulting in an initial radius of 8 mm and a thickness of 2.5 mm. Briefly, cells were pelleted and resuspended by subsequent additions of the following solutions: 5X DMEM (CellGro), phenol-red free growth media, FBS, 0.1 N NaOH and 4 mg/ml acid-solubilized bovine collagen type I stock (MP Biomedicals, Solon, OH) at ratios of 2:1:1:1:5, respectively, resulting in a 2 mg/ml collagen solution with SC. Growth factor reduced Matrigel™ (BD Biosciences) was the final component incorporated- as it gels much more rapidly than the collagen- at 10%, 20%, 35%, or 50%, by volume. Dilution with Matrigel™ at these percentages reduced the collagen I concentration to 1.8, 1.6, 1.3, and 1.0 mg/ml, respectively; constructs without any Matrigel™ retained the collagen I concentration of 2 mg/ml. In some cases, the growth factors TGF-β1 (R&D Systems, Minneapolis, MN) or IGF-1 (Sigma) were incorporated at 2 ng/ml or 5 ng/ml, respectively, in collagen only gels as controls. Construct solutions were mixed using a micropipettor , transferred into well plates, and placed at 37°C for 30 min to cause gelation. Constructs remained fully hydrated during this time, and subsequently were covered by 1 ml phenol red free growth media and loosened from the sides of the wells using a sterile plastic spatula. All constructs were cultured for 3, 7, or

14 days prior to analysis, with the media being changed every 2 days. No compaction was observed in any of the constructs over 14 days in culture.

2.3.3 Second Harmonic Generation (SHG) and Scanning Electron Microscope (SEM) Imaging

For SHG imaging, constructs were washed in phosphate buffered saline (PBS, Cambrex, Walkersville, MD) and fixed for 30 min at room temp using a 4% paraformaldehyde (Sigma)/4% sucrose (Sigma) solution. Samples were visualized using a laser scanning confocal microscope (Carl Zeiss, Thornwood, NY) equipped with a Ti-Sapphire femto-second pulsed laser (Coherent, Inc. Santa Clara, CA) at 63x magnification. The laser was tuned to 820 nm and a bandpass filter of 390-465 nm was employed to visualize the collagen networks.[105]

Constructs were prepared for SEM by an initial fixation in a 2% glutaraldehyde (Poly Scientific, Bay Shore, NY)/2% paraformaldehyde solution for 1 hr. Following a PBS wash, samples were exposed to serial dilution in increasing percentages of ethanol, up to 100%. Samples were critically point dried using an Autosamdri-815 (Tousimis Research Corp., Rockville, MD) and sputter coated with platinum for visualization. All SEM imaging (Carl Zeiss SMT, Thornwood, NY) was performed on day 3 at magnifications of 25,000x.

2.3.4 Compliance Testing

Acellular composite constructs were prepared at 0%, 10%, 20%, 35%, and 50% Matrigel™ (n=3 for each condition). The matrix bulk stiffness describes the mechanical properties the cells will experience when embedded in the constructs. Unconfined compression testing was performed on day 3 using an EnduraTEC ELF 3200 system (Bose Corp., Eden Prairie, MN) equipped with a 250 g load cell and a 1.27 cm^2 Lexan platen. Constructs remained in medium at 37°C until testing commenced. The construct was brought up to the compression platen by eye and the load cell tared. Under displacement control, a constant strain rate of 0.5 mm/min was applied and the resulting force (in N) was measured every 200 msec. From these data, stress vs. strain curves were created. All stresses below 0.4 kPa were eliminated as these were assumed to be due to negligible interaction forces before the platen touched the surface of the gel. The strain

was normalized to reflect this change. The linear region of the resulting curve was determined to be between 15% and 50% of the maximal strain. The slope of this linear region was calculated and the resulting elastic moduli graphed.

2.3.5 Cell Viability and Number

Cell viability and cell number in each construct were quantified after 3, 7, and 14 days in culture. Viability was analyzed using a vital dye kit (Molecular Probes, Carlsbad, CA). Constructs were washed in PBS then stained concurrently with calcein (1:1000) and ethidium homodimer (EH, 1:500) diluted in PBS for 45 minutes followed by two PBS washes to remove excess dye. Live (calcein+) and dead (EH+) cells were visualized using a laser scanning confocal microscope (Carl Zeiss) equipped with 488 nm and 543 nm lasers and a 10x objective. 150 μm z-stacks were taken of each sample and subsequently analyzed using FARSIGHT software, which can segment and count cells.[106] Z-stacks were taken of both sides of the constructs and the location of image stacks was the same for all construct conditions to control for possible differences in diffusion characteristics. Total numbers of live cells and dead cells were tabulated for each construct type and output as a percentage of living cells (living cells/total cells). Three separate trials were performed, testing one of each construct type per trial.

Cell number was quantified using the CyQuant GR Cell Proliferation Kit (Molecular Probes). Whole constructs (n=4 per construct type) were frozen at -80°C and subsequently freeze dried using a Labconco Freeze Dry system (Labconco Corporation, Kansas City, MO). Lyophilized constructs were digested with a Proteinase K solution (Sigma) for 16-20 hours at 55°C and digested samples were frozen at -20°C for at least 24 hours to help ensure cell lysis, as CyQuant GR is a membrane impermeable DNA stain. 50 μl of each sample was then combined with 150 μl CyQuant GR dye solution in 1X cell lysis buffer to yield a final dye concentration of 1X. Samples were loaded into a 96 well plate along with cell standards ($6.25x10^4$-$1.00x10^6$ cells/ml) and DNA standards (2-30 μg/ml), incubated in the dark for 5 minutes, and read using a fluorescence plate reader (Bio-Tek, Winooski, VT) set at 485 nm excitation and 528 nm emission. Fluorescence intensity was correlated to DNA and cell standards in order to estimate the number of cells within each construct.

2.3.6 Cell Morphology

Cell morphology was assessed both qualitatively and quantitatively at days 3, 7, and 14. Samples were fixed and permeabilized in 0.1% Triton X-100 (Sigma). The actin network was visualized using Alexa Fluor 488-conjugated Phalloidin (Molecular Probes) diluted 1:100 in 1% bovine serum albumin (Sigma) for 30 min. Nuclei were stained with ethidium homodimer (Molecular Probes) diluted 1:500 in PBS for 20 min. Constructs were washed twice and visualized on a laser scanning confocal microscope (Carl Zeiss) using 488 nm and 543 nm lasers at 20x magnification. Z-stacks ranging from 50-90 μm thick were taken of the interior of each construct, again imaging both sides and keeping z-stack locations consistent for all conditions.

2.3.7 Image Analysis

Neurolucida software (MBF Biosciences, Williston, VT) was used to identify individual nuclei and to trace actin in 3D space. Preliminarily, in order to correlate actin to cell morphology, low density SCs on tissue culture treated glass coverslips were stained and imaged for actin. Additional phase microscopy images were taken at the same locations to visualize cell morphology. Tracings of actin networks via Neurolucida (described below) and tracings of the whole cell were then plotted to compare size and shape, demonstrating that actin networks were an accurate estimation of cell morphology (0.92 correlation factor). This step was necessary since it is much easier to visualize actin in 3D constructs than it is to visualize cell membrane boundaries.

In 3D constructs, Neurolucida traces were used to quantify the length and number of branches of the actin networks (n=3 replicates of each construct type- at least 6 image stacks for each replicate were analyzed). Any partial cells were disregarded so that only cells which could be traced in their entirety were analyzed. Although much of the Neurolucida tracing is automated, some user intervention was required when two actin networks were intimately touching one another. In this case, actin tracings were manually separated at a distance halfway between the two nuclei containing each of the actin networks. It should be noted that this underestimates the absolute length since it is likely that the tracings actually overlap one another. Even though the absolute length could not be accurately ascertained, since this convention was upheld over the course of

all tracings and construct types, relative measurements were still valid. Neurolucida Explorer was used to automatically analyze the average actin process length and number of processes for each full cell within an image stack; in this work a cell process was defined as a protrusion from the SC.

2.3.8 Statistics

One-way ANOVA was used to detect if any significant differences existed between groups in a dataset and Tukey's multiple comparisons test was subsequently used to evaluate all pairwise comparisons. Significance was set at a p-value below 0.05.

2.4 Results

2.4.1 Matrix Composition

Second harmonic generation imaging revealed varied collagen I distribution within the different construct types (Fig. 1 a-e). Collagen I autofluorescence is shown in red and a dense network of uniformly distributed fibrils, which is a triple helix of collagen I protein chains, could be seen within the 100% collagen constructs (Fig. 1 a). This dense network was notably absent as the Matrigel™ percent increased to 35% and 50% (Fig. 1 d,e). In these constructs the collagen I appeared less interconnected and less uniformly distributed throughout, forming distinct islands of higher collagen concentrations amidst the Matrigel™. 10% (Fig. 1 b) and 20% (Fig. 1 c) Matrigel™ constructs showed a progression from the dense network of fibrils seen in the collagen only constructs to the clustering of collagen I present in the 35% and 50% Matrigel™ conditions.

SEM images also illustrated differences in matrix structure. Again, in the collagen only matrix, a dense network of highly interconnected collagen Type I fibrils could be visualized (Fig, 1 f). Upon incorporation of 10% Matrigel™ (Fig. 1 g), this well defined network disappeared, replaced instead by tightly packed fibrils with fewer and smaller pores. As the percentage of Matrigel™ increased from 20% to 35% to 50% (Fig. 1 h-j, respectively) fibrils and pores again began to appear within the matrices. However, these fibrillar networks looked distinctly different from those seen in the collagen only constructs. SEM imaging, however, cannot definitively identify collagen I fibrils in a Matrigel™ matrix. Fibrils here formed a less interconnected network and appeared more

tortuous in nature. Additionally, regions of fibrils containing relatively large pores could be seen adjacent to areas of tightly packed matrix, reminiscent of that seen in the 10% Matrigel™ constructs. Accurate quantification of pore size was difficult in these samples due to changes in construct volume during the drying process. However, since this effect was constant over all conditions, relative comparisons were valid.

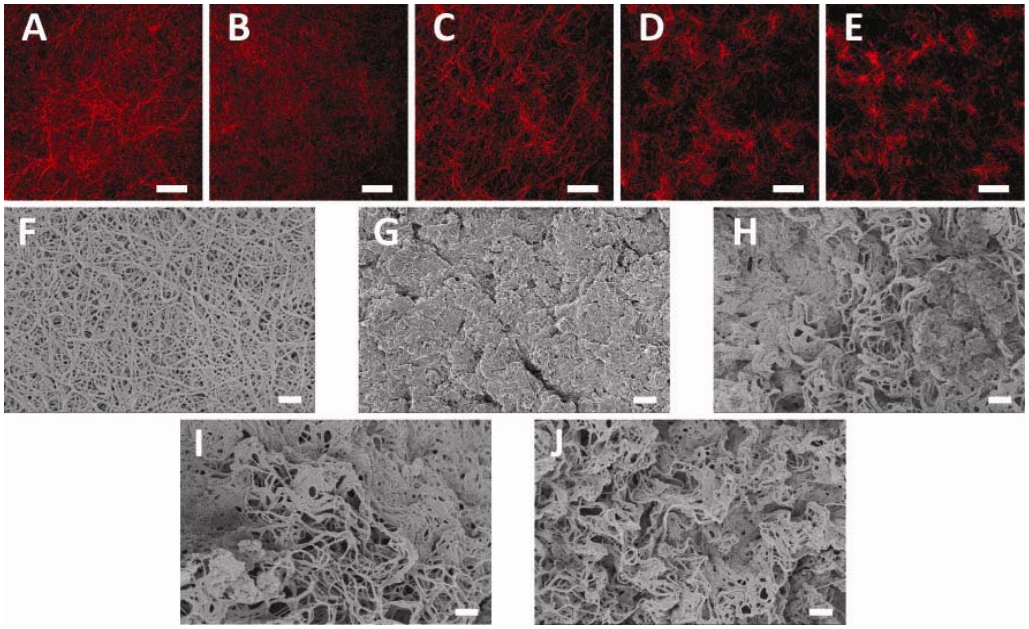

Figure 1: SHG and SEM Images. (A-E) Second harmonic generation images of the collagen Type I network within (A) collagen only, (B) 10% Matrigel™, (C) 20% Matrigel™, (D) 35% Matrigel™, and (E) 50% Matrigel™ constructs. Collagen Type I autofluorescence is shown in red and is distributed non-uniformly in the higher percent Matrigel™ constructs resulting in regions with greater relative concentrations of collagen Type I or Matrigel™ proteins. Images are 2D projections of 15 μm thick z-stacks. Scale bars: 20 μm, 63x magnification. (F-J) SEM images of (F) collagen only, (G) 10% Matrigel™, (H) 20% Matrigel™, (I) 35% Matrigel™, and (J) 50% Matrigel™ constructs. Scale bars: 1 μm, 25,000x magnification.

2.4.2 Compliance Testing

Acellular constructs were subjected to compression testing and exhibited differences in mechanical properties. The stiffest construct was the 50% Matrigel™, exhibiting an elastic modulus of 9.8 kPa (Fig. 2). A reduction in Matrigel™ resulted in a linear decline in modulus, with the 10% Matrigel™ being most compliant at 5.1 kPa. The collagen only construct had a slightly higher modulus of 6.4 kPa. Statistical differences were

detected among all groups ($p < 0.001$) except between the 20% Matrigel™ and collagen only constructs, as these conditions had similar moduli of 6.6 kPa and 6.4 kPa, respectively.

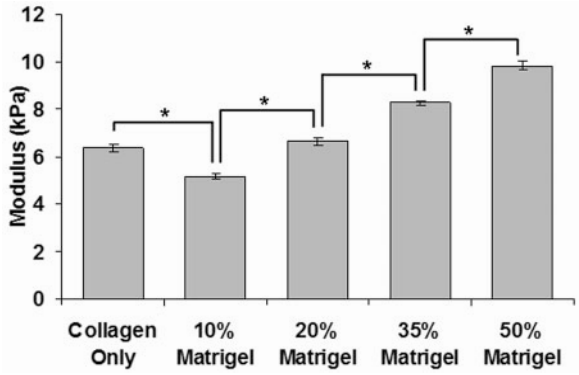

Figure 2: Young's moduli of the various collagen-Matrigel™ compositions. Moduli were obtained through displacement control unconfined compression at a rate of 0.5 mm/min. Moduli were calculated from the linear region of the stress-strain curve which was assumed to be between 15% and 50% of the maximal stress. Following an initial drop in elastic moduli, constructs became increasingly stiffer with the addition of Matrigel™. Bars are mean ± SE. * indicates significant statistical differences ($p < 0.05$). n=3 separate trials.

2.4.3 Cell Viability

Cell viability was measured using vital cell dye and expressed as the percentage of living cells on days 3, 7, and 14 (Fig. 3 a). Viability was above 90% for all construct types on days 3 and 7 and no differences were detected between any of these groups. By day 14, SC viability within the collagen only, 2 ng/ml TGF-β1, and 5 ng/ml IGF-1 constructs dropped to 70%, 81%, and 77%, respectively. Any constructs containing Matrigel™ retained viability values over 93% on day 14, which were significantly higher than the collagen only constructs with and without added growth factors ($p < 0.05$). The vital cell dye was functional since dead cells were observed in all samples. Notably, viability was constant regardless of the location within the construct.

2.4.4 Cell Number

Cell number in constructs was estimated by total DNA using the CyQuant GR DNA assay on days 3, 7, and 14 (Fig. 3 b). $5x10^5$ cells were incorporated into each construct on day 0 and this number was not exceeded on any day. No significant differences

between groups were detected on day 3. By day 7, 35% and 50% Matrigel™ constructs has significantly more cells than collagen constructs with and without growth factors; no differences were detected between Matrigel™ containing constructs on day 7.

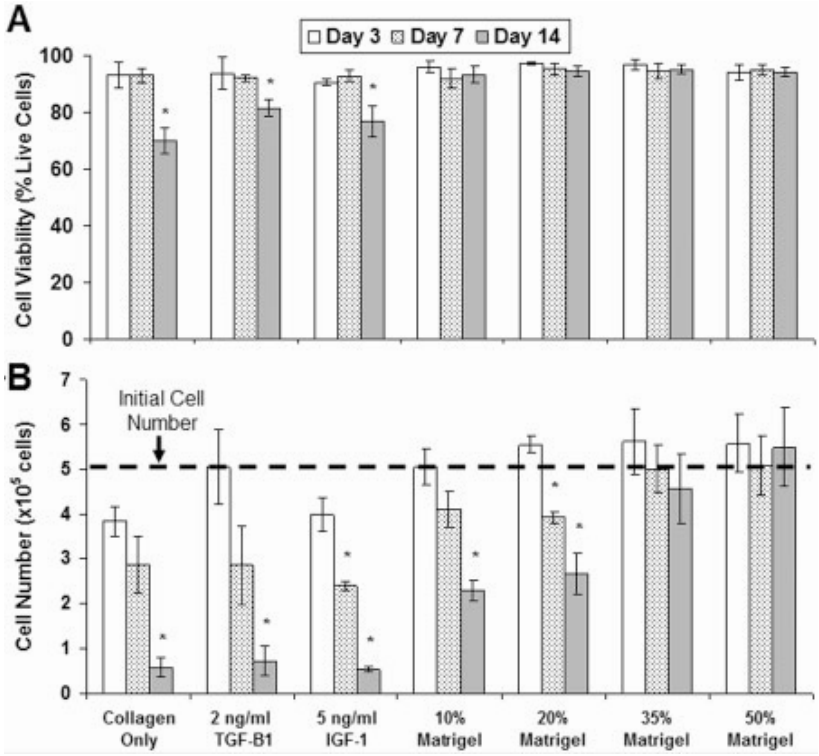

Figure 3: Schwann cell viability and number in 3D. (A) Cell viability on days 3, 7, and 14 in culture, displayed as the percentage of living cells. Live and dead cells were stained using calcein and ethidium homodimer, respectively, and analyzed using FARSIGHT software. Cell viability was above 90% for all constructs on days 3 and 7. On day 14, only constructs containing Matrigel™ had viabilities above 90%. (B) Cell numbers assessed at days 3, 7, and 14 via a DNA assay. Initial seeding density was 5x105 cells/construct and after 14 days in culture, increasing percentages of Matrigel™ correlated to higher cell numbers. 50% Matrigel™ constructs supported the highest number of cells at 14 days with 5.4x105 cells/construct while collagen only constructs averaged 5.8x104 cells; an 88% decrease from the initial cell seeding number. Bars are mean ± SE. * indicates a significant decrease from the day 3 value for each condition ($p < 0.05$). n=3 trials for viability data and n=4 for cell number data.

By day 14, the increase in cell number correlated to the increase in Matrigel™ percent was much more pronounced. The 35% and 50% Matrigel™ constructs had significantly higher cell numbers than any other constructs ($p < 0.05$). After 14 days in culture, although cell number was highest in the 50% Matrigel™ construct, no

significant difference in number was detected between the 35% and 50% Matrigel™ conditions when compared to the day 3 values; all other constructs had significantly fewer cells at day 14 than at day 3 ($p < 0.05$). Neither IGF- nor TGF-β1 increased cell number when compared to collagen only controls over 14 days in culture.

2.4.5 Cell Morphology

Cell morphology was examined via actin networks on days 3, 7, and 14 for all construct types. Actin networks, shown in Fig. 4 as 2D projections of 3D image stacks, were traced and analyzed as an indicator of cell morphology. Preliminarily, SC were cultured on glass coverslips and whole cell spreading (whole cell tracing in phase micrographs) was correlated (0.92 correlation factor) to the tracing of actin in fluorescence micrographs, indicating that actin was an accurate estimation of SC size and shape (data not shown).

Within the collagen only constructs, a spherical SC morphology was observed (Fig. 4 a) and the addition of neither TGF-β1 nor IGF-1 elicited dramatic changes in morphology, although a few small processes can be seen protruding from these cells (Fig. 4 b,c, respectively); resulting in 1.4-fold and 1.2-fold increases in average process length, respectively, when compared to collagen only controls (Fig. 5 a). However, the incorporation of Matrigel™ resulted in significant changes in cell morphology. All constructs containing Matrigel™ had significantly higher average process lengths ($p < 0.001$), with the 10%, 20%, 35% and 50% constructs achieving 2.4, 3.5, 3.7, and 4.2-fold increases in average process length over collagen only controls (Fig. 5 a). Even at 10% Matrigel™, numerous thin processes extended from the cell body (Fig. 4 d) with an average of 3.8 processes per cell. Although these processes were significantly shorter, more processes per cell were present when compared to all other conditions ($p < 0.001$). As the percentage of Matrigel™ was increased from 20% to 35% to 50% (Fig. 4 e-g, respectively) processes became noticeably longer and straighter, with fewer processes present on each cell within the higher percent Matrigel™ constructs (Fig. 5 b). Despite this, no significant changes in number of processes per cell were detected between these groups and only the 20% and 50% Matrigel™ constructs differed significantly with each other with respect to average process length ($p < 0.001$). Collagen only constructs and

collagen constructs with TGF-β1 or IGF-1 contained an average of 2.4, 2.2, and 2.3 small processes per cell (Fig. 5 b), respectively, and these differed significantly from the 10% Matrigel™ condition only ($p < 0.001$). It is important to point out that data for days 3, 7, and 14 were pooled together for each construct type, as no differences in morphology were detected between days, indicating that cell spreading occurred within 3 days in culture. Additionally, cell morphology was consistent throughout the volume of each construct. Over 14 days, processes were longest in the 50% Matrigel™ constructs, although differences when compared to the 35% Matrigel™ condition were not significant.

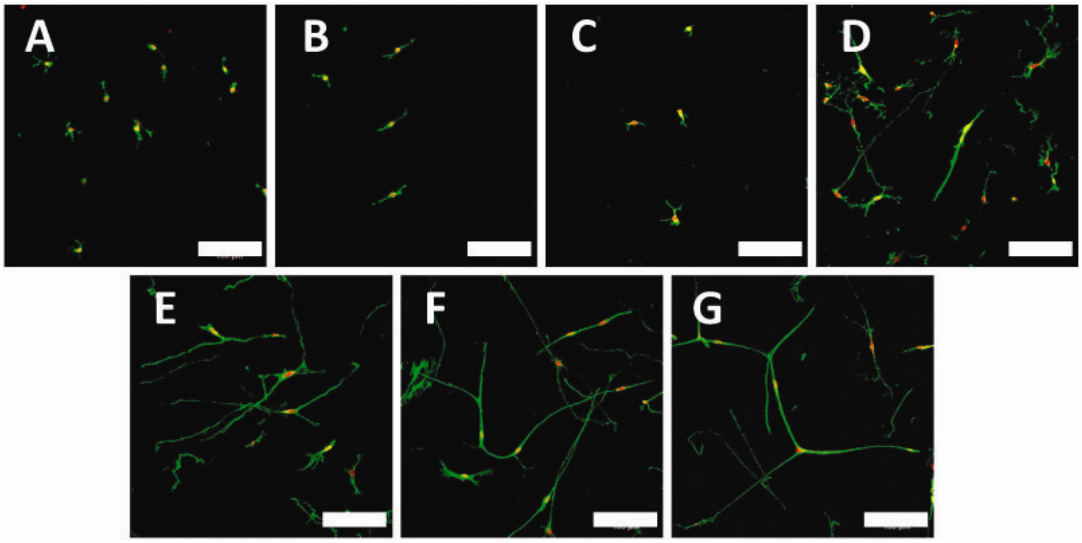

Figure 4: Schwann cell morphology within the various constructs. Cells within the (A) collagen only constructs were spherical in morphology and those cells in the (B) collagen only constructs with 2 ng/ml TGF-β1 or (C) 5 ng/ml IGF-1 extended a limited number of very short processes. Thin but longer processes appeared upon the incorporation of (D) 10% and (E) 20% Matrigel™. These processes became visibly longer and straighter as the Matrigel™ percentage was increased to (F) 35% and (G) 50%. Actin was stained green using Alexa-Fluor 488-conjugated phalloidin and nuclei were stained red via ethidium homodimer. Images are 2D projections of 40 μm z-stacks obtained using a confocal microscope. Scale bars: 100 μm, 20x magnification.

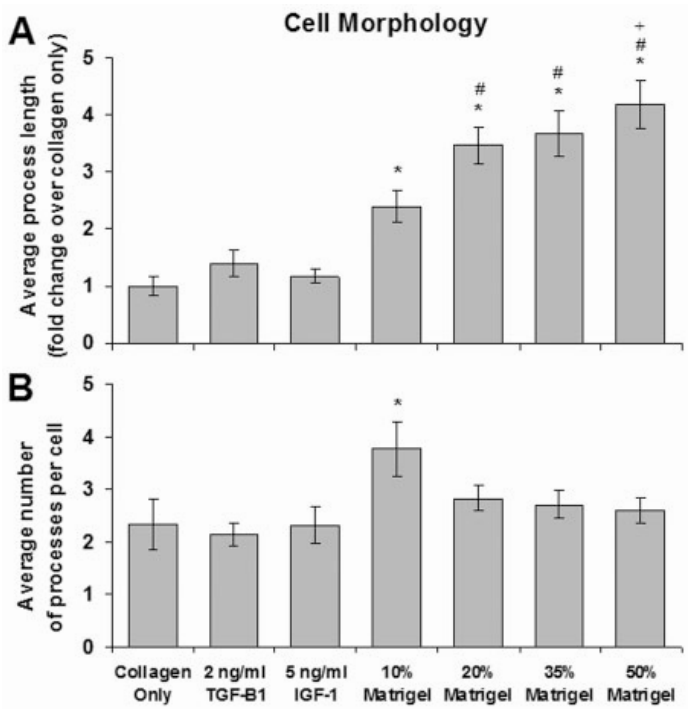

Figure 5: Schwann cell morphology in 3D. (A) Average process length and (B) average number of processes per cell. Actin networks stained using Alexa fluor 488-conjugated phalloidin were traced and analyzed using Neurolucida software. Values were averaged over 14 days in culture for each construct type. Process length increased with the percentage of Matrigel™ reaching a 4.2-fold increase over the collagen only condition in the 50% Matrigel™ case. The number of processes increased significantly in only the 10% Matrigel™ case where there was an average of 3.8 processes/cell. Bars are mean ± SE. *, #, and + indicate significantly greater than collagen control, 10%, and 20% Matrigel, respectively ($p < 0.05$). n=3 separate trials with 6 images stacks being analyzed for each condition in each trial (~10 cells/image stack).

2.5 Discussion

This study lays a foundation for our long term goal of achieving directed neuronal regeneration. Scaffolds for nerve repair are typically optimized for neurite growth while the glial response to the materials is less well studied. In this study, we have taken an alternate approach by creating materials that additionally support Schwann cells. As discussed, SC possess the ability to support and can direct neurite growth and our overall aim is to use oriented SC in a 3D in vitro matrix environment to promote and guide neurite extension. Achieving this effect requires that SC interact with the matrix such that they survive and elongate. By using 3D collagen-Matrigel™ composite scaffolds,

we have created mechanically robust materials that allow SC extension and therefore may have utility in directing neurite outgrowth.

SHG imaging revealed the distinct structural differences between the various matrix types examined in this study and portrayed the distribution of the collagen I amid the Matrigel™. Collagen I has a triple-helix structure and a high degree of crystallinity making it visible to SHG.[105] Additionally, strong chiroptical properties enhance its autofluorescence. These chiroptical properties are not present in collagen IV or laminin, and therefore these proteins are not visualized using SHG imaging.[107] Brown, *et al.* reported no SHG activity from Matrigel™ proteins using SHG settings very similar to those in this study.[108] Therefore, we are confident that the autofluorescence viewed in our samples was a result of the fibrillar collagen I distribution.

Collagen I is a mechanically robust structural protein, and its distribution affects the mechanical structure and resulting strength of the bulk material. *In vitro,* collagen constructs are easily handled, which is an issue of practical importance when contemplating their use as engineered tissues in the clinic. In addition, previous work has demonstrated that the collagen fibrils within constructs can be directionally aligned using a variety of techniques.[109, 110] Matrix alignment offers the possibility of creating SC outgrowth in prescribed directions and will also promote associated aligned neurite outgrowth. For these reasons, collagen I was used as the primary matrix material for the constructs in this study.

Incorporation of Matrigel™ caused distinct changes in the mechanical properties and structure of the constructs, while also altering the cellular response. Addition of Matrigel™ resulted in more fragile constructs, although all compositions used in this study were robust enough to be handled without damage. Constructs containing more than 50% Matrigel™ could not be practically handled without tearing, and were therefore not investigated further. Constructs with higher Matrigel™ content may have ripped more easily because the highly interconnected collagen fibril network seen in pure collagen constructs was disrupted, replaced instead by islands of collagen (Fig. 1 e). At low Matrigel™ concentrations (e.g. 10%, Fig. 1 g), the matrix structure as observed by SEM was uniform with a fine fiber structure, while at higher percentages of Matrigel™ larger fibrils reappeared (Fig. 1 h-j). It is likely that the observed fibrils are

collagen domains amid more compact Matrigel™ matrix, however SEM imaging does not allow us to reliably distinguish between these proteins. The observed changes in fibrillar structure are also supported by Fig. 2; the addition of Matrigel™ initially resulted in a decreased modulus compared to collagen controls yet further addition of Matrigel™ ultimately yielded constructs with moduli which exceeded those of collagen controls. Additionally, SHG images (Fig. 1, which image only the fibrillar collagen structure) support the SEM observations, showing domains of collagen I at higher Matrigel™ concentrations. The incorporation of Matrigel™ clearly altered the mechanical and architectural properties of the matrices, though the mechanism of this effect requires further study.

Compliance of a substrate directly affects the phenotype of cells that are in contact with it.[111, 112] Previous research has shown the importance of mechanical stiffness in neural tissue engineering; for instance, Leach *et al*., demonstrated that branching of PC12 neurites decreased on compliant materials below a certain threshold.[97] Much of the published work, however, has involved quantifying neurite outgrowth, rather than glial cell morphology.[96, 113] It is interesting to note that in our study there was a direct correlation between increased stiffness and SC spreading, with the stiffer constructs inducing a greater degree of spreading. Nevertheless, we were not able to discriminate between the effects of the mechanical properties and the biological effects of the protein components in the Matrigel™. It is important to note that the pure collagen samples had moduli that were not significantly different from the 20% Matrigel™ samples, yet SC spreading was clearly different between these constructs (Fig. 4 a,e). Even though the 10% Matrigel™ samples were significantly more compliant than the pure collagen constructs, increased spreading was still observed in the presence of Matrigel™. These results suggest that matrix compliance is not the only factor affecting SC extension, and that the biological cues from Matrigel™ also contribute.

Cell viability in all constructs was high, though there were significant drops at day 14 in culture in the pure collagen and collagen with TGF-β1 or IGF-1. Cell number in the 3D constructs tended to increase with increasing Matrigel™ content, especially at the later time points. For anchorage-dependent cell types, inhibition of cell spreading has been shown to trigger apoptosis.[114] Chen, *et al.* reported that cell shape governed

whether individual cells grew or died and that when cell shape and spreading were sufficiently restricted, apoptosis was induced.[115] Additionally, Nakao, *et al.* reported that over 50% of harvested SC undergo apoptosis after losing contact with axons but these SC could be rescued from apoptosis by increasing their adhesion using different substrata.[116] These results suggest that a lack of cell adherence to the matrix, and the associated lack of cell spreading, was responsible for cell death in the constructs with lower Matrigel™ content. Viability data showed that the cells that remained in the constructs were viable, though the cell number data demonstrate that there were fewer of them as the amount of Matrigel™ decreased. Since viability data are only a snapshot in time, it is likely that dead cells degraded over time, and therefore only viable cells remained at longer time points. Our results show that the 35% and 50% Matrigel™ scaffolds were most supportive of cell maintenance over 14 days in culture.

The main extracellular matrix proteins in the nervous system in contact with SC-axon units are the basal lamina proteins laminin and collagen IV. Collagen I is not a major protein in contact with these cells as it lies outside the basal lamina in the endoneurium.[83] Therefore it is likely that the addition of Matrigel™ allowed SC to preferentially attach to the proteins of their native environment and extend processes in the composite matrices used in this study. Addition of Matrigel™ to a construct necessarily results in a corresponding decrease in collagen I content (since all constructs were made at the same total protein content). However, we verified that SC extension was independent of the collagen I concentration by creating controls with variable collagen I content (1.0-2.0 mg/ml collagen) in the absence of Matrigel™. These collagen concentrations corresponded to the concentrations achieved by the addition of the various levels of Matrigel™ in this study. Regardless of the collagen I concentration, SC remained in a spherical morphology in the absence of Matrigel™. Additionally, we did not observe any increase in SC survival by lowering the collagen I concentration. Matrix compliance may have played a role in determining the degree of SC extension, but our overall our data suggest that the addition of Matrigel™, and not the decrease in collagen I, was responsible for cell spreading.

Addition of exogenous TGF-β1 at 2 ng/ml or IGF-1 at 5 ng/ml to collagen I constructs did not elicit cell spreading at a level comparable to that achieved by the

addition of Matrigel™. Previously, it has been reported that TGF-β1 caused SC to spread within collagen I matrices at concentrations as low as 0.5 ng/ml.[86] This work, however, classified cells as either spread or unspread based on the presence or absence of cellular processes, respectively, and consequently expressed cell spreading as the percentage of cells classified as containing processes. In the current work, we quantified the length of processes and not the percentage of cells adopting a spread morphology, making direct comparisons difficult. We did, however, observe a 1.4-fold increase in average process length with the addition TGF-β1 compared to collagen only controls (Fig. 5 a) and small processes could be seen protruding from many of the cells in TGF-β1 containing constructs (Fig. 4 b). Therefore, TGF-β1 at 2 ng/ml did have some effect in changing cell morphology although the addition of Matrigel™ resulted in substantial changes. It should be noted that TGF-β1 and IGF-1 are the only growth factors which are not effectively eliminated in the growth factor reduced formulation of Matrigel™, and are present at concentrations of ~1.7 ng/ml and ~5 ng/ml, respectively.[87] Since we observed little increase in cell spreading with the exogenous addition of either of these growth factors to collagen I constructs, it is likely that process extension is occurring due to the presence of laminin and collagen IV in the Matrigel™ mixture, proteins typically found in the basal lamina.

These results show that Schwann cell morphology and behavior in a 3D matrix is altered by the relative amounts of collagen Type I and Matrigel™ in composite scaffolds *in vitro*. Collagen I and Matrigel™ both have desirable properties for use in creating engineered neural tissues: collagen I is a mechanically robust protein which can be directionally aligned, while Matrigel™ can provide a suitable environment for SC adhesion and extension. Additionally, each material has been used previously in both the PNS and CNS *in vivo* and have shown to be permissive to neurite extension.[59, 76, 84, 95] However, use of these proteins separately is not suitable in creating a neural guidance scaffold because SC spreading and growth are not observed in pure collagen constructs, while pure Matrigel™ constructs are mechanically fragile and do not contain robust fibers for alignment. The composite constructs we studied retained positive properties of each component, although these properties changed with the relative concentrations of the protein components. In future work, we will use these composite protein scaffolds in

conjunction with scaffold alignment, soluble factors, and external forces to promote and direct the extension of neurites and migration of SC through the scaffold biomaterial. The potential synergy of multiple cues presented to the supporting SC and regenerating axons may lead to a clinically effective scaffold for injuries to the nervous system.

3. Chapter 3: Development of a Stable, Aligned, Schwann Cell Loaded Scaffold for Neural Engineering

3.1 Abstract

The purpose of this work was to develop and characterize a 3-D, Schwann cell (SC) loaded collagen I-Matrigel scaffold to serve as a platform for studying the effects of cell and matrix alignment on neurite outgrowth. Here, we sought to create a stable, aligned matrix with no external tension using fibroblast (FB) mediated constrained compaction. While in constraint, SC and FB aligned in the direction of constraint. Once cut from constraint, both cell types reoriented perpendicular to their original direction after 2 days and retained this new alignment for 7 days. These compacted, oriented scaffolds are supportive of directed neurite outgrowth. In future work, these stable, aligned matrices will be used to examine the individual and synergistic effects of multiple guidance cues on 3-D neurite outgrowth.

3.2 Introduction

Spatially organized tissue is a hallmark of a number of organ systems and neural tissue is no exception.[117] Following injury, the regenerating axons need to reconnect to their innervation target to ensure the injured neuron is properly supported. Failure to re-connect to the target would result in death of the neuron. Guidance of the regenerating axons provides a more direct path across the injury site and decreases the time for functional recovery.[118] Scaffold alignment is one factor that has been used to direct axons and a number of studies have demonstrated the beneficial effects which alignment has on *in vitro* and *in vivo* neurite outgrowth.[84, 89, 93] *In vitro,* aligned Schwann cells (SC) have a demonstrated ability to direct neurite outgrowth[75] and an aligned SC topography alone has shown to be sufficient to promote neuronal adhesion and orient neurites.[90] *In vivo* aligned collagen I constructs have demonstrated utility in enhancing repair of both peripheral and central nerve defects.[84, 88, 93] Aside from the *in vivo* applications, aligned 3D scaffolds present a unique opportunity to study the effects different guidance cues have on neurite outgrowth.

Creating stable, aligned constructs is something which can be done a number of different ways ranging from magnetic orientation[84] to mechanical stimulation[119] to

electrical stimulation.[110] One approach to aligning tissue is to use fibroblast (FB)-mediated constrained compaction. It is known that FB will spontaneously compact and reorganize collagen I when cultured in a 3D environment and it has been demonstrated that, when grown in a constrained environment, FB are able to align collagen I along the axis of constraint.[92] A benefit of this method is that is uses only cell-based mechanisms to align the tissue, limiting the inclusion of other variables. However, the application of constraint requires the addition of an external apparatus not feasible for use *in vivo* and adds the additional variable of tension to the system, which complicates studies concerning the effects of specific guidance cues on neurite outgrowth.

The purpose of this work is to develop a stable, aligned scaffold from a collagen I-Matrigel™ biomaterial using FB-mediated constrained compaction as the only means of alignment. This aligned material could then be used to examine 3D neurite outgrowth in the presence of multiple guidance cues such as aligned cells, aligned matrix, gradients of soluble factors, electrical stimulation and mechanical forces. In doing so, the relative and synergistic strengths of each cue may be better understood for the rational design of a scaffold to assist in the repair of spinal cord and large-gap peripheral nerve repair. Here, we sought to culture SC and FB in a model composite matrix comprised of collagen I-Matrigel™ and monitor cell and matrix alignment under constraint and following removal of constraint. Pilot studies demonstrated that these aligned Schwann cell–fibroblast composite constructs supported and directed neurite outgrowth.

3.3 Materials and Methods

3.3.1 Cell Culture

Primary SC were isolated from the sciatic nerves of neonatal rats using a previously described procedure.[120] Subsequent expansion and culture of SC was carried out in Dulbecco's Modified Eagle's Medium containing 4 mM L-glutamine, 4.5 g/L D-glucose, 110 mg/L sodium pyruvate (DMEM; CellGro, Manassas, VA) and supplemented with 10% fetal bovine serum (FBS; HyClone, Logan, UT), 50 U penicillin/streptomycin (Cellgro), 10 μg/ml bovine pituitary extract (BPE; Becton, Dickinson and Company, Franklin Lakes, NJ), and 10 μM forskolin (Sigma-Aldrich, St. Louis, MO). Cells were grown at 37°C and 7% CO_2 with the media being changed every

other day. SC between passages 6-10 were used for all experiments and prior to use, SC purity was assessed in monolayer culture using S100 staining and quantified using ImageJ (NIH). Purity levels of >95% were observed for all cultures from passages 6-10.

Primary FB were isolated from the skin of neonatal rats using a 1 mg/ml collagenase, 0.1% trypsin solution followed by a subsequent 0.25% trypsin digestion. FB culture was carried out in DMEM containing 4 mM L-glutamine, 4.5 g/L D-glucose, 110 mg/L sodium pyruvate (CellGro) and supplemented with 10% FBS (HyClone) and 50 U penicillin/streptomycin (Cellgro). Cells were grown at 37°C and 7% CO_2 with the media being changed every other day.[103] Cells were passaged at ~90% confluence using a 0.05% trypsin/0.53 mM EDTA solution (CellGro) and only cells from p5-p15 were used for all experiments.

3.3.2 Construct Formation

To prepare cells for use in constructs cells were first trypsinized for 5 min. Following trypsinization, SC and FB were separately diluted in growth medium and pelleted. Each cell type was then suspended in 5 ml phenol-red free SC growth media (CellGro) to reduce background fluorescence;[104] aside from the absence of phenol red, this growth media was identical to the SC media described above. SC media was effectively used for the culture of both cell types as SC media is FB media with added BPE and forskolin to specifically promote SC proliferation. Prior to use in constructs, both cell types were separately counted, partitioned, and pelleted again prior to use. Pellets of SC and FB could then be combined to achieve the desired cell ratios.

Cell pellets of SC and/or FB were then resuspended by subsequent additions of the following solutions: 5X DMEM (CellGro), phenol-red free growth media, FBS, 0.1 N NaOH and 4 mg/ml acid-solubilized bovine collagen type I stock (MP Biomedicals, Solon, OH) at ratios of 2:1:1:1:5, respectively, resulting in a 2 mg/ml collagen solution with SC and/or FB, depending on the condition. Growth factor reduced Matrigel™ (BD Biosciences) was the final component incorporated- as it gels much more rapidly than the collagen- at 35% by volume. 35% Matrigel™ was chosen for use because this concentration of Matrigel™ has shown to be supportive of SC and neurons while remaining relatively mechanically robust. Incorporation of 35% Matrigel™ by volume

resulted in a final collagen I concentration of 1.3 mg/ml. Construct solutions were mixed using a micropipettor to ensure a more homogenous distribution of the matrix, transferred into the proper plates, and placed at 37°C for 30 min to cause gelation. Constructs remained fully hydrated during this time, and subsequently were covered by 1 ml phenol red free SC growth media and loosened from the sides of the wells using a sterile plastic spatula. Constructs were cultured for up to 14 days prior to analysis, with the media being changed every 2 days.

Three different construct variations were prepared in this study: 1) unconstrained FB only, 2) unconstrained SC and FB, and 3) constrained SC and FB. To investigate FB proliferation in the 3D matrices, unconstrained, FB only constructs were prepared in 24 well plates at 0.5 ml and seeded at a density of $2.5x10^5$ FB/ml. This is the same FB density used for constrained constructs. Use of these plates resulted in an initial scaffold radius of 8 mm and a thickness of 2.5 mm. To examine the compaction profile of unconstrained constructs, SC and FB were incorporated into 0.5 ml scaffolds also prepared in 24 well plates. SC density was held constant at $2x10^6$ SC/ml while FB density was varied from $4x10^4$-$2x10^6$ FB/ml.

Based on the results from the FB proliferation and scaffold compaction studies, 0.5 ml constructs in a constrained well were prepared containing both SC and FB at densities of $2x10^6$ and $2.5x10^5$ cells/ml, respectively. The aseptic constrained well, as shown in figure 6 below, consisted of a polydimethlysiloxane (PDMS) exterior (Fig. 6A), which served to create the walls of the well. PDMS was used to form the wells as it is a non-cytotoxic polymer which is easily cast in a variety of shapes and sizes. Cells will also not adhere to untreated PDMS. The well shape was cut out using a scalpel and two triangular shaped pieces of porous polypropylene (Fig. 6B) were inserted at each end of the channel. When the construct solution (Fig. 6D) was poured into the well, it became integrated into the porous plastic, allowing FB mediated compaction to only happen in two dimensions (Fig. 6C); the other dimension of compaction was into the page. Therefore, the porous polypropylene served to constrain the scaffold at two ends. Following 3 or 7 days of constrained compaction, constructs were cut from constraint by severing each end of the construct adjacent to the polypropylene. Cut constructs were then transferred to a regular 24 well plate and cultured for up to 7 more days.

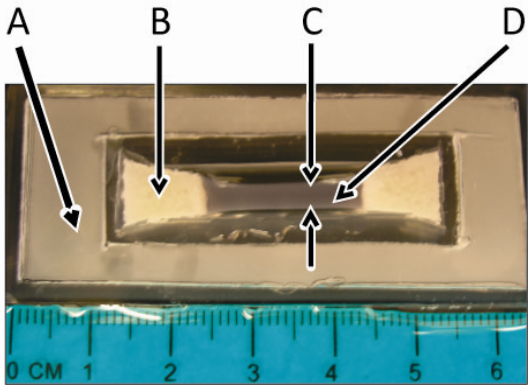

Figure 6: Schematic of the constrained well. (A) constrained well containing a (D) SC and FB loaded construct. (B) Porous polypropylene served to constrain the construct at each end so that (C) compaction could only happen in two dimensions. Following up to 7 days of constraint, constructs were cut from the well by severing the scaffold adjacent to the polypropylene.

3.3.3 Gel Compaction Profile

To examine the effect of the SC:FB ratio on matrix compaction, constructs were made containing $2x10^6$ SC/ml and between $4x10^4$ and $2x10^6$ FB/ml. Constructs were cultured for 7 days and a digital photograph was taken of each construct replicate (n=3 replicates of each) on each day. Gel volume was quantified by tracing construct perimeters using NIH ImageJ which yielded the compacted area of the construct. Compaction was assumed to be equal in all directions since no constraint existed is this system, so the compacted area was used to calculate a corresponding change in height. Finally, the volume change of the construct was expressed a percentage of the original volume (all constructs were initially created at the same size).

3.3.4 Fibroblast Proliferation Analysis

FB only constructs were created to analyze the 3D proliferation of FB over 14 days in culture. Briefly, at days 0, 1, 2, 3, 7, and 14 constructs initially seeded with $2.5x10^5$ FB/ml were removed from well plates and cell number was analyzed using the CyQuant GR Cell Proliferation Kit (Molecular Probes). Whole constructs were frozen at -80°C and subsequently freeze dried. Lyophilized constructs were digested with a Proteinase K solution (Sigma) for 16-20 hours at 55°C and digested samples were frozen at -20°C for at least 24 hours to help ensure cell lysis, as CyQuant GR is a membrane

impermeable DNA stain. 50 µl of each sample was then combined with 150 µl CyQuant GR dye solution in 1X cell lysis buffer to yield a final dye concentration of 1X. Samples were loaded into a 96 well plate along with cell standards ($6.25x10^4$-$1.00x10^6$ cells/ml) and DNA standards (2-30 µg/ml), incubated in the dark for 5 minutes, and read using a fluorescence plate reader (Bio-Tek, Winooski, VT) set at 485 nm excitation and 528 nm emission. Fluorescence intensity was correlated to DNA and cell standards in order to estimate the number of cells within each construct.

3.3.5 Cell Alignment

Following 7 days of unconstrained culture, 3-7 days of constrained culture only, or 3-7 days of constrained culture followed by an additional 1-7 days of unconstrained culture after constraint was removed, constructs were fixed and analyzed for cell and matrix alignment. Samples were fixed for 30 min at room temperature and subsequently permeabilized using a 0.1% Triton X-100 solution (Sigma). Given the dense, compacted nature of these constructs, staining was difficult and inefficient if the constructs were not first sectioned into thin slices prior to applying antibodies. Sectioning was done with the use of a dissecting microscope and a razor blade and slices of construct were cut in directions both parallel and perpendicular to the long axis of the construct. By imaging sections of construct perpendicular to one another, any range of cellular orientation could be visualized

After sectioning, constructs were first incubated with a rabbit anti-S100 antibody (Dako, Denmark) diluted to 1:400 in 3% bovine serum albumin (BSA) for 1 hr at room temperature to specifically tag Schwann cells. Following three 5 min rinses a secondary antibody, Alexafluor 546-conjugated goat anti-rabbit diluted 1:1000 in HBSS, was applied for 1 hr to fluorescently tag the primary antibody. Subsequently, a mixture of Alexafluor 488-conjugated phalloidin diluted 1:100 and DAPI diluted 1:1000 in 1% BSA was applied to fluorescently tag actin and nuclei, respectively. Constructs were visualized on a laser scanning confocal microscope (Carl Zeiss) using 405 nm, 488 nm, and 543 nm lasers at 15x magnification. Z-stacks ranging from 60-80 µm thick were taken of the interior of each construct. Images were consistently taken of at least two

planes of the construct to ensure all cellular orientations were captured. Additionally, all images were taken as close to the center section of the construct as possible.

In addition to imaging cellular alignment, the alignment of collagen I fibrils was also examined. Second harmonic generation (SHG) imaging was used to visualize collagen fibrils. Constructs were prepared in the same manner as for immunohistochemistry, minus the application of staining antibodies. Samples were visualized using a laser scanning confocal microscope (Carl Zeiss) equipped with a Ti-Sapphire femto-second pulsed laser (Coherent, Inc.) at 20x magnification. The laser was tuned to 820 nm and a bandpass filter of 390-465 nm was employed to visualize the collagen networks.

3.3.6 Neuron Plugs

To examine the ability of these constructs to support 3D neurite outgrowth, plugs of neurons were created in unaligned, uncompacted matrices containing SC only and also in aligned, compacted matrices containing both SC and FB. In both cases, prior to adding neurons, constructs were created as before and cultured for 7 days in a constrained or unconstrained fashion. After 7 days, a sterile 2 mm dermal punch was used to punch a hole in each of the constructs, with the aid of a dissecting microscope. Collagen I-Matrigel™ solutions were then prepared as described with the omission of SC and FB. Instead, dissociated neurons isolated from neonatal rat DRG, were incorporated into the construct mixture at $2x10^6$ cells/ml. 5 µl of this solution was then used to fill the holes created with the dermal punch. After allowing for gelation (30 min) constructs were covered with SC media supplemented with 75 ng/ml NGF and cultured for an additional 3 days. Following culture, fixation, staining, and imaging were performed as described with the only addition being that neurons were stained for β-III-tubulin concurrently with the S100 SC staining. β-III-tubulin primary and secondary antibodies were applied at concentrations of 1:400 and 1:1000, respectively.

3.3.7 Statistics

One-way ANOVA was used to detect if any significant differences existed between groups in a dataset and Tukey's multiple comparisons test was subsequently used to evaluate all pairwise comparisons. Significance was set at a p-value below 0.05.

3.4 Results

3.4.1 Gel Compaction Profile: Variable SC:FB Ratio

To examine the effect which the SC:FB ratio has on the compaction profile of the gel, FB number in unconstrained constructs was varied from $4x10^4$-$2x10^6$ FB/ml, while the SC number was held constant at $2x10^6$ SC/ml. This resulted in SC:FB ratios ranging from 50:1 to 1:1. Intermediate ratios included 2:1, 4:1, 6:1, 8:1, and 20:1. After 7 days in culture, not surprisingly, the constructs containing the highest number of FB (1:1 ratio) compacted to approximately 7% of their initial volume.

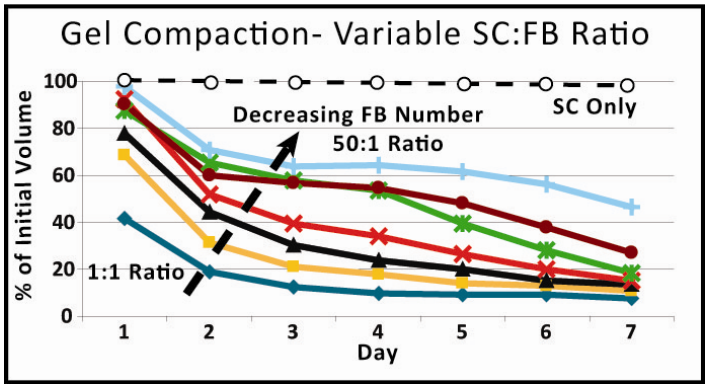

Figure 7: Gel compaction expressed as a percentage of the initial construct volume. Constructs with a 1:1 SC:FB ratio (bottom line) compacted most while constructs with the fewest FB (top line) compacted the least. Compaction appears to reach a plateau of around 7% of initial volume for most groups after 7 days in culture.

By day 7, no significant differences in compaction percent were detected between the 1:1 constructs and constructs with ratios up to 8:1 (green line in Fig. 7). After 7 days in culture, compaction appeared to plateau for nearly all groups, reaching a maximum of around 7% of the initial volume. In related work, the SC number was varied while the FB number was held constant and compaction was equal for all groups. Additionally, SC

alone in these matrices do not compact it to any degree, as shown in Figure 7, indicating that FB number regulates the amount of compaction .

3.4.2 Fibroblast Proliferation

FB number was examined over 14 days in culture using the CyQuant GR Cell Proliferation Assay. An initial significant drop in cell number was observed following 3 days in culture ($p<0.05$) compared to the day 0 seeding density of $2.5x10^5$ FB/ml (Fig. 8). However, between days 3 and 7, FB number increased steadily reaching a value of $3.8x10^5$ FB/ml, significantly more than the initial seeding value ($p<0.05$). Over the next 7 days in culture, FB number remained relatively steady, appearing to plateau at a value of around $3.8x10^5$ FB/ml. No significant change between the day 7 and day 14 values was detected. This plateauing of cell number by 7 days corresponds to the timing of the compaction plateau observed in the variable SC:FB ratio compaction experiment.

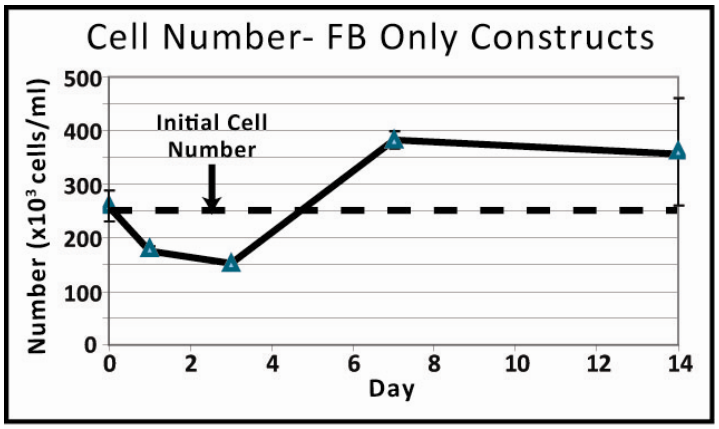

Figure 8: FB number in collagen I-Matrigel™ scaffolds. Initially FB number decreases over 3 days but steadily rises between days 3 and 7, reaching a plateau of around 3.8x105 FB/ml. This number was maintained for at least an additional 7 days in culture. Error bars represent standard error of the mean.

3.4.3 Cell and Matrix Alignment and Realignment

Alignment of cells and matrix (collagen I) was visualized after both constrained and unconstrained compaction and the results are displayed in Figure 9. All images displayed were taken in the longitudinal plane of the construct, which is depicted in Fig. 9M. Schwann cells were labeled with S100, a characteristic SC marker (red), and phalloidin

was used to label actin of all cells, predominately identifying the fibroblasts (green). Following 7 days of unconstrained compaction both SC and FB appear disorganized and randomly oriented throughout the composite matrix material (Fig. 9A). Additionally, no apparent alignment of the collagen I fibrils is observed in SHG imaging (Fig. 9E). However, after 7 days of constrained compaction (Fig. 9B), both cells types become oriented in the direction of constraint and fibrillar orientation in this direction can be observed as well (Fig. 9F). This orientation in the direction of constraint occurred as early as 3 days, but appeared stronger after 7 days (data not shown). During this initial period of constrained compaction, constructs compacted in two dimensions only, as they were unable to contract the gel in the direction constrained by the porous polypropylene. Once removed from constraint, cells and matrix again became disorganized, losing their longitudinal alignment after just 1 day of unconstrained compaction (Fig. 9C and 9G). However, 2 days following removal from constraint, a realignment of cells and matrix was observed in a direction perpendicular to the initial alignment (Fig. 9D and 9H). Notably, this realignment was also perpendicular to the new direction of compaction, which is consistent with the initial longitudinal alignment which occurred during constrained compaction. This realignment, however, consistently occurred in the vertical dimension only, which should be noted is the smallest dimension of the scaffold.

Even 4 and 7 days post-cutting, this vertical orientation of cells and matrix remained and appeared even more pronounced than that observed 2 days post-cut (Fig. 9I-L). This phenomenon was consistently repeated over four separate trials when 7 days of initial constrained compaction was allowed for. Interestingly, if constructs were cultured under constraint for only 3 days as opposed to 7, inconsistent realignment was observed. Sometimes constructs would realign, as is always the case when 7 days of constrained compaction is first performed. However, frequently these constructs would not realign at all. It is interesting to highlight that 7 days of initial constrained compaction corresponds to both the compaction and FB number plateaus observed in the initial work. Regardless, if 7 days of initial constrained compaction is performed followed by removal of constraint and subsequent unconstrained culture, both cells and matrix realign in a direction perpendicular to their original alignment, and always in the vertical dimension.

This vertical alignment is stable for the duration of 2-7 days following removal from constraint.

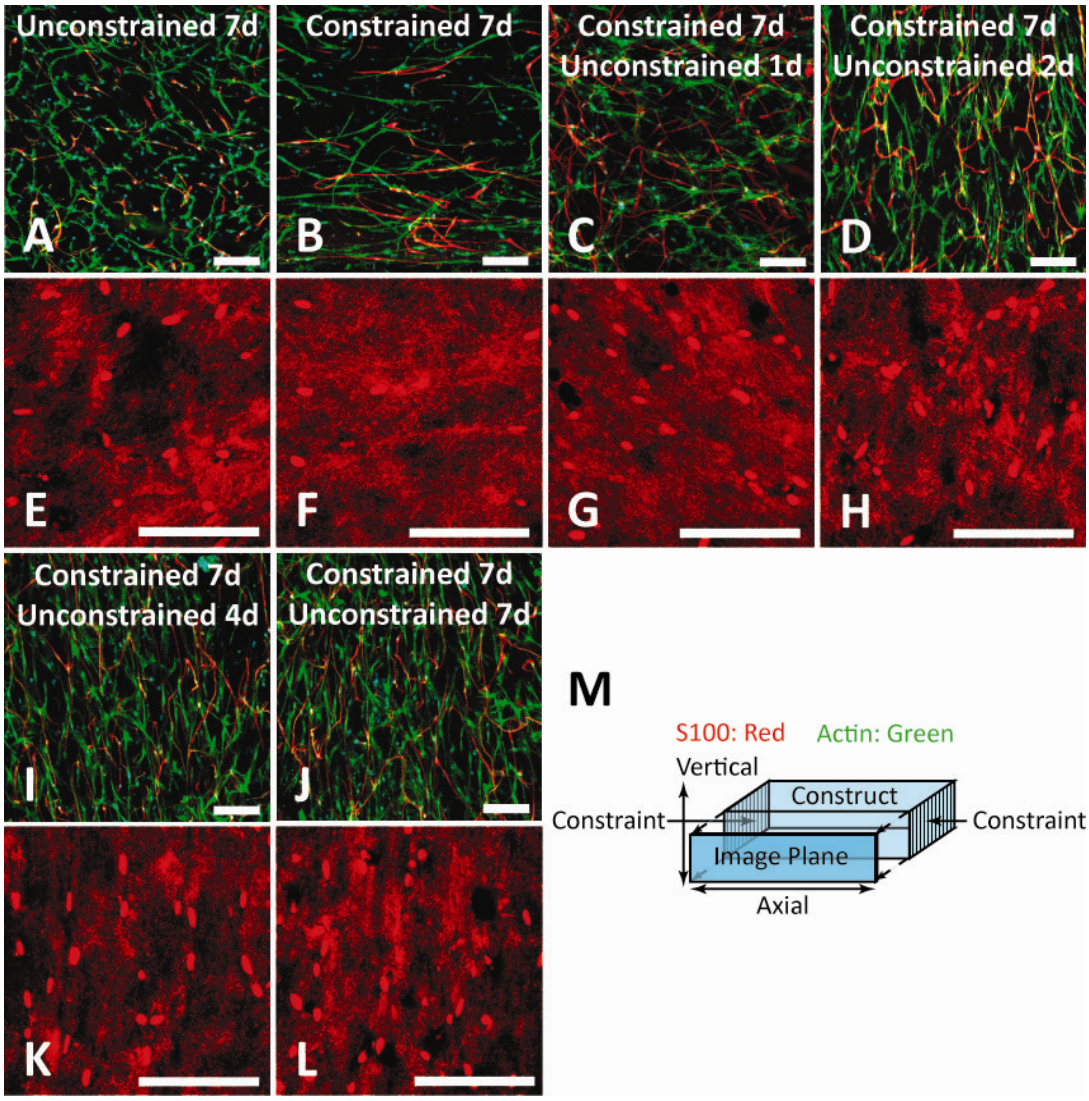

Figure 9: Alignment of cells and matrix following constrained and unconstrained compaction. Actin is displayed in green while S100 is red (images A-D, I, J). Collagen I fibrils are visualized in (E-H, K, L) using SHG imaging. Both cells and matrix show a realignment perpendicular to their initial longitudinal alignment following removal of constraint and this alignment remains stable over 7 days in culture. Scale bars represent 100 μm.

3.4.4 Neurite Outgrowth in Aligned Constructs

In pilot studies, neurite outgrowth was examined in the aligned compacted SC/FB composite scaffolds. Briefly, scaffolds were punched with a 2 mm dermal punch and a plug of dissociated neurons in collagen I-Matrigel™ was added to the void. Neurite outgrowth was examined after 3 days in culture. Results are displayed in Figure 10.

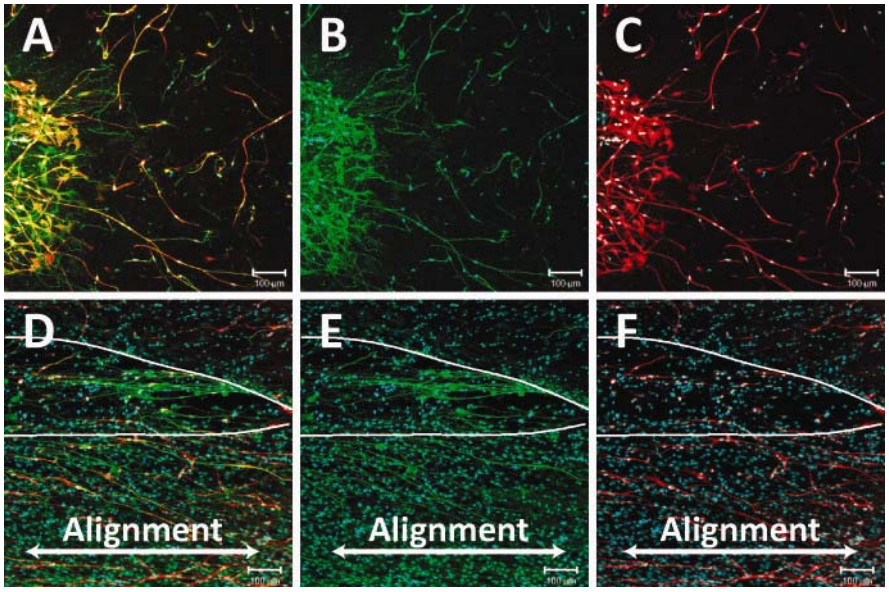

Figure 10: Neurite outgrowth in aligned and unaligned constructs. (A-C) unaligned, uncompacted constructs and (D-F) aligned, compacted constructs. (A,D) Show concurrent S100 (red) and B-3-tubulin (green) staining while (B,E) are the B-3-tubulin components only, showing neurite outgrowth, and (C,F) are the S100 components only, showing SC after 3 days in culture. The white outline in D-F represents the plug boundary. Scale bars are 100 μm.

Neurite outgrowth was examined in both unaligned, uncompacted (Fig. 10A-C) and aligned, compacted constructs (Fig. 10D-F). In the unaligned, uncompacted constructs, neurites, labeled with β-III-tubulin (green), can be seen leaving the plug and entering the SC loaded matrix (Fig. 10B). Often, these neurites leaving the plug are in close proximity with SC, as evidenced by the overlap of the red and green channels in Fig. 10A. Neurite outgrowth from the plug in unaligned constructs does not appear biased in any direction. In constructs aligned using FB mediated compaction, it can be seen that SC are aligned in a longitudinal direction, as evidenced by the left-to-right orientation of

these cells (Fig. 10F). Neurites, shown in green, can be seen leaving the plug boundary, outlined in white, and following the direction of alignment (Fig. 10E). This outgrowth is both 3D in nature and oriented with the observed cell and matrix alignment. Collectively, this demonstrates that not only are these constructs supportive of 3D neurite outgrowth, but aligned cell and matrix components are sufficient to cause oriented neurite outgrowth.

3.5 Discussion

We have demonstrated the ability to create stable, aligned collagen I-Matrigel™ constructs using FB mediated compaction and these aligned constructs were shown to be stable for a minimum of 7 days in unconstrained culture. These aligned constructs will have utility in examining neurite outgrowth in a 3D model under variable conditions, such as an aligned matrix, aligned cells, neither, or both. Presumably, cells could be lysed following alignment so that only an aligned matrix remains. Additionally, aligned constructs such as these may serve as a platform for the incorporation and subsequent investigation of the effects of a host of different guidance cues on 3D neurite outgrowth (soluble factors, scaffold composition, cells, and external forces (electrical and mechanical). Work presented in this thesis demonstrated that, not only are these constructs supportive of 3D neurite outgrowth and Schwann cells, but aligned cell and matrix components are able control the direction of neurite outgrowth, which is highly relevant to the field of neural tissue engineering.

It is known that FB compact collagen I and therefore it is believed that FB reorganize the collagen fibrils in response to constraint, aligning the matrix and subsequently the SC as well. It was noted in this study that, if only 3 days of initial constrained compaction were allowed for, inconsistent realignment results were achieved, something not seen when 7 days of initial constraint was performed. This can be explained by the FB number and compaction profiles observed in this work. FB number is more than 2-fold lower at day 3 than at day 7 within these constructs. Clearly, this indicates that substantial FB proliferation is occurring between days 3 and 7, until it reaches a plateau, potentially an upper bound of the number of cells which the construct can support, at day 7. If the constructs are cut while the FB are in this highly

proliferative phase (i.e. day 3), the cells may have a decreased ability to reorganize the matrix material in response to the removal of constraint and hence, reproducible realignment is not observed.

At 3 days, even with the highest number of FB, compaction has yet to reach a plateau. In fact, for the 8:1 SC:FB ratio used in the realignment studies, compaction does not plateau until approximately day 6. During the initial constrained compaction period, compaction is allowed to happen in only two dimensions because of the constraint. If this initial compaction is allowed to reach a plateau, which takes around 6 days, constructs will no longer compact in these dimensions when removed from constraint. Essentially, this creates another form of constrained compaction even after constructs are cut from the porous polypropylene. Since they are fully compacted in the first two dimensions, compaction is only allowed to proceed in 1 dimension when constraint is removed, and this may be the factor responsible for the stable realignment of the matrix and cells. If only 3 days of initial constraint is allowed for, compaction in the first two dimensions is likely to be incomplete upon removal of constraint. As a result, compaction will then proceed in all three dimensions when constraint is removed, decreasing the realignment effect. For this reason, it is necessary to allow for 7 days of initial compaction, or at least allow for compaction to plateau in the first two dimensions, for a consistent realignment effect to be observed.

Another interesting facet of this study is that realignment of the cells and matrix consistently occurred in the vertical direction, as opposed to the horizontal direction. Both these orientations are perpendicular to the initial longitudinal alignment of the cells and matrix so it seems likely that either one of them, or both, may occur following removal of constraint. This however, was not the case as horizontal alignment was never observed; instead cells always oriented vertically. Construct geometry may be used in part to explain this phenomenon. As the system is set up, the vertical dimension of the constructs is the smallest dimension. It is believed that FB show preference to reorient in this dimension as it offers the path of least resistance to reorganization. Collagen fibrils would have to be oriented over longer distances if the horizontal alignment was adopted which would require more work and a greater coordinated effort.

Diffusion limitations within the constructs may also play a role in the preference for vertical reorganization. Given the density of the constructs, it is feasible that a nutrient gradient may be established through the vertical dimension of the scaffold since the constructs remain stationary while in constraint. While constrained, the forces generated by the constraint could be sufficient to overcome any alignment effects caused by a nutrient gradient. When constraint is removed, this gradient may be sufficient to then "persuade" the cells to reorganize in the vertical dimension as opposed to the horizontal dimension. One pitfall to this explanation, however, is that realignment persists and is stable for at least 7 days in culture. Upon removal of constraint, constructs freely float in media and a directed nutrient gradient should be abolished by this effect. If anything, a radial gradient would be expected whereas nutrient concentrations would be equal on all surfaces and decrease towards the center. This would lend no preference to a vertical reorganization. As such, this supports the notion that it is the construct geometry and not an effect of nutrient transport responsible for the consistent vertical reorganization of the cells. In any case, future studies will involve investigating the effects of variable construct geometries on cell and matrix realignment.

As a first step for the construction of a novel biomaterial for neural engineering, SC migration and neurite extension within the scaffolds were preliminarily examined. Both these aspects would be crucial to the development of an effective biomaterial. Neurite extension is necessary for reconnections with host tissue to form and SC migration is required for myelination during regeneration.[121] Additionally, it is hypothesized that directionally migrating SCs could be used to further enhance directed neurite outgrowth. As seen in figure 10, neurites are able to extend outwards within the composite matrices. Additionally, plugs of SC placed within acellular collagen I-Matrigel™ composite constructs (not shown) were able to migrate outwards through the scaffold material. Presumably, pore sizes within the matrix are large enough to allow for both neurite extension and SC migration, meeting two necessary requirements for a neural engineering biomaterial.

Other studies have investigated the use of aligned collagen I for nerve repair with promising results, albeit full functional recovery was not achieved. In one study, collagen I fibrils were aligned in a magnetic field and then implanted into a 6 mm rat

sciatic nerve defect.[84] Although directed axon outgrowth was increased when compared to controls without implanted collagen, insufficient myelination of axons was observed. In order to achieve full functional recovery, myelination is essential as it speeds the conduction of action potentials.[67] One reason which could account for the lack of myelination is that SC were unable to migrate in the collagen only graft. It has been documented that SC adopt a spherical morphology within collagen I and, as such, these cells may have been unable to follow the extending neurites and perform the necessary process of myelination.[86] The constructs presented within this thesis aim to alleviate this problem through the creation of an environment supportive of SC and neurons. SC survive better in these composite biomaterials than in collagen I alone and adopt a spread morphology not seen in collagen I. SC in collagen I-Matrigel™ composite biomaterials have the ability to migrate and in future studies, this may prove to be beneficial in the myelination of axons regenerating through the graft.

Stable, aligned constructs such as the ones created in this work may have utility in a number of applications. Here, these constructs are intended for neural engineering applications and studying the effects of variable guidance cues on 3D neurite outgrowth. However, by altering the cellular components, these stable, aligned constructs may be applied to other fields as well. Organized tissue is a hallmark of a number of organ systems and consequently, constructs similar to the ones created here have potential uses in areas such as cardiovascular engineering, tendon and ligament repair, and skin repair, among others. Nonetheless, this work has presented a method for creating stable, aligned constructs using only cellular machinery. These aligned constructs have demonstrated utility in directing 3D neurite outgrowth and future work will involve investigating this outgrowth in the presence of multiple cues such as aligned cells, aligned matrix, soluble cues, and applied electric fields.

4. Chapter 4: Discussion and Conclusions

This work has described the creation of a novel biomaterial comprised of collagen I and Matrigel™ intended for neural engineering applications. The overall goal of this project is to develop a therapeutically effective scaffold for the treatment of spinal cord injury and large-gap peripheral nerve repair. Toward this goal, it is important to understand how different guidance cues affect neurite outgrowth so that an implantable biomaterial can be optimized with these guidance cues in mind. Guidance cues such as chemical cues[21, 94, 95], physical cues[74, 90], cellular cues[75, 81], substrate specific cues[88, 96, 97], mechanical cues[98], and electrical cues[99, 100] all are well documented as having an effect on neurite outgrowth. However, a gap in knowledge exists as to how these cues may synergistically interact. Given the complexity of the injury environment, it is likely that a treatment for SCI will involve a multifaceted approach using number of different guidance cues, thereby substantiating the importance of understanding synergistic interactions amongst these cues.

A specific contribution of work presented in this thesis is the establishment of a platform for studying these interactions amongst variable guidance cues. In the first part of this thesis, a biomaterial consisting of 65% collagen I and 35% Matrigel™, by volume, was developed and characterized. This biomaterial was developed to be specifically supportive of both SC and neurons, as it has been reported that collagen I alone, a material frequently used in guidance channel studies, is not readily supportive of SC despite its support of neurite outgrowth.[86] It is likely that a material concurrently supportive of glial and neuronal cells will offer improved results over a material optimized solely for neurite outgrowth, as SC have been closely linked to nerve regeneration and play an important role in myelinating the axons.[68]

The second part of this thesis sought to stably align the cellular and matrix components of this biomaterial and examine neurite outgrowth within the 3D environment. Alignment has implications in guidance of neurites[18, 40, 84, 85] and is an important cue to investigate in the development of a graft material. Stable, aligned constructs were created through the use of FB mediated constrained compaction. Following an initial period of 7 days of constraint, cells and matrix reorganized in a direction perpendicular to their original alignment once cut from the constrained model.

This new alignment was preserved for at least 7 days in culture without the application of any external forces. Importantly, it was confirmed that neurites were able to extend into these matrices and directed 3D outgrowth was observed in the presence of aligned cells and matrix. Other work using aligned collagen I matrices have failed to examine cell or matrix alignment after the initial alignment period.[84, 85, 93] Work presented within this thesis confirms that stable aligned constructs containing aligned SC have been created and that this material is supportive of 3D Schwann cell spreading and migration.

In turn, this model biomaterial motivates a larger study to investigate a more complete determination of an optimal biomaterial that is optimized to support the ascending and descending tract, interneurons, re-vascularization and the glia needed to re-myelinate the regenerated axons. In this work, we spent some time optimizing materials for Schwann cells and sensory neurons, but there are many ECM and matrix components that we were not able to screen as it was beyond the scope of the project. Matrigel™ is not a material that can be used for clinical trials due to its production by mouse tumor cells. Additionally, testing a host of ECM components at the macro-scale, as done in this work, is both time and labor intensive. If similar constructs are brought down to the micro-scale, a wider range of ECM proteins can be examined in the search for a truly optimized biomaterial. Work contained within this thesis, however, clearly highlights the need for material optimization as substantial changes in SC survival and morphology were observed simply by the addition of Matrigel™ to collagen I. Future studies may aim to increase proliferation of SC within these biomaterials as the current scaffolds were only able to maintain SC number in culture, not increase it. SC proliferation is likely to be beneficial because as more and more regenerating axons populate an injury site, more SC will be required for myelination. Vasculature is also required for a fully functional therapeutic treatment and this aspect of graft design was not investigated in this work. As a therapeutic cure for SCI moves closer to realization, the problem is likely to get even more complex with the addition of factors such as vasculature. Given this, revision and vigorous research into material optimization will be essential, and this thesis motivated the optimization of biomaterials for neural engineering,

Using this biomaterial as a model material, the individual and synergistic effects of multiple guidance cues on neurite outgrowth can be examined in 3D, a more realistic recapitulation of the *in vivo* microenvironment. Neurite outgrowth in the presence of an aligned matrix and/or cells can be examined. Lysing the cellular component of the biomaterial following alignment would result in solely an aligned matrix. In this manner, the specific effect of SC alignment can be examined. In addition, other cues aside from cell and matrix alignment could be incorporated into these matrices. Growth factors such NGF, NT-3, and BDNF could be applied in conjunction with alignment or released in a spatially, time-dependent pattern. Potential for observed synergy on neurite outgrowth is promising as all these neurotrophic factors have shown to enhance neurite outgrowth.[18] Additionally, a neurotrophic factor such as glial growth factor 2, known to increase SC motility[94], could be applied in efforts to increase SC migration through the biomaterial, with the hypothesis that this would further promote directed neurite outgrowth.

Electric fields could also be applied through the construct material. Electric fields have been implicated in both astrocyte and SC alignment and directed migration.[122, 123] Electric field induced alignment and migration of glia has shown promise in directing neurite outgrowth[99] yet the synergistic effects of directed SC migration in an aligned 3D scaffold remain less studied. If necessary, electrically conductive carbon nanotubes could be added to the scaffold to increase the electrical conductivity as well.[92]

Ultimately, the scaffolding material described here may be used to help fill the knowledge void existing between the known neurite guidance cues and the specific and synergistic effects of each. *In vitro* models, such as the ones presented in this thesis afford more detailed analysis of cell behavior and have a higher through-put to test a wider array of conditions for a more focused animal study. Spinal cord injury is an immensely complex injury and as such, a full understanding of the microenvironment conditions and guidance cues present is necessary. By establishing a platform allowing for the incorporation of multiple guidance cues at one time, this complete understanding may be better realized and cue presentation can be optimized. It is the intent that a biomaterial such as the one developed here may eventually contribute a therapeutic cure for SCI. Fully understanding guidance cue interactions *in vitro* will lead to more efficient graft materials *in vivo*.

5. Chapter 5: Literature Cited

1. National Spinal Cord Injury Statistical Center. Spinal Cord Injury Facts & Figures at a Glance 2008. Birmingham, AL, 2008. http://www.spinalcord.uab.edu/. Date last accessed: 6 May 2009.

2. Guth, L., Barrett, C.P., Donati, E.J., Anderson, F.D., Smith, M.V., and Lifson, M. Essentiality of a specific cellular terrain for growth of axons into a spinal cord lesion. Exp Neurol 88, 1, 1985.

3. Freund, P., Schmidlin, E., Wannier, T., Bloch, J., Mir, A., Schwab, M.E., and Rouiller, E.M. Nogo-A-specific antibody treatment enhances sprouting and functional recovery after cervical lesion in adult primates. Nat Med 12, 790, 2006.

4. David, S., and Aguayo, A.J. Axonal elongation into peripheral nervous system "bridges" after central nervous system injury in adult rats. Science 214, 931, 1981.

5. Windle, W.F., and Chambers, W.W. Regeneration in the spinal cord of the cat and dog. J Comp Neurol 93, 241, 1950.

6. Fitch, M.T., and Silver, J. Activated macrophages and the blood-brain barrier: inflammation after CNS injury leads to increases in putative inhibitory molecules. Exp Neurol 148, 587, 1997.

7. Silver, J., and Miller, J.H. Regeneration beyond the glial scar. Nat Rev Neurosci 5, 146, 2004.

8. Zhang, H., Uchimura, K., and Kadomatsu, K. Brain keratan sulfate and glial scar formation. Ann N Y Acad Sci 1086, 81, 2006.

9. Apostolova, I., Irintchev, A., and Schachner, M. Tenascin-R restricts posttraumatic remodeling of motoneuron innervation and functional recovery after spinal cord injury in adult mice. J Neurosci 26, 7849, 2006.

10. Jones, L.L., Margolis, R.U., and Tuszynski, M.H. The chondroitin sulfate proteoglycans neurocan, brevican, phosphacan, and versican are differentially regulated following spinal cord injury. Exp Neurol 182, 399, 2003.

11. Rhodes, K.E., and Fawcett, J.W. Chondroitin sulphate proteoglycans: preventing plasticity or protecting the CNS? J Anat 204, 33, 2004.

12. Pindzola, R.R., Doller, C., and Silver, J. Putative inhibitory extracellular matrix molecules at the dorsal root entry zone of the spinal cord during development and after root and sciatic nerve lesions. Dev Biol 156, 34, 1993.

13. Xie, F., and Zheng, B. White matter inhibitors in CNS axon regeneration failure. Exp Neurol 209, 302, 2008.

14. Kerschensteiner, M., Schwab, M.E., Lichtman, J.W., and Misgeld, T. In vivo imaging of axonal degeneration and regeneration in the injured spinal cord. Nat Med 11, 572, 2005.

15. Tom, V.J., Steinmetz, M.P., Miller, J.H., Doller, C.M., and Silver, J. Studies on the development and behavior of the dystrophic growth cone, the hallmark of regeneration failure, in an in vitro model of the glial scar and after spinal cord injury. J Neurosci 24, 6531, 2004.

16. Davies, S.J., Goucher, D.R., Doller, C., and Silver, J. Robust regeneration of adult sensory axons in degenerating white matter of the adult rat spinal cord. J Neurosci 19, 5810, 1999.

17. Fitch, M.T., and Silver, J. CNS injury, glial scars, and inflammation: Inhibitory extracellular matrices and regeneration failure. Exp Neurol 209, 294, 2008.

18. Stichel, C.C., and Muller, H.W. Experimental strategies to promote axonal regeneration after traumatic central nervous system injury. Prog Neurobiol 56, 119, 1998.

19. Benowitz, L.I., and Routtenberg, A. GAP-43: an intrinsic determinant of neuronal development and plasticity. Trends Neurosci 20, 84, 1997.

20. Herdegen, T., Skene, P., and Bahr, M. The c-Jun transcription factor--bipotential mediator of neuronal death, survival and regeneration. Trends Neurosci 20, 227, 1997.

21. Weidner, N., Blesch, A., Grill, R.J., and Tuszynski, M.H. Nerve Growth Factor–Hypersecreting Schwann Cell Grafts Augment and Guide Spinal Cord Axonal Growth and Remyelinate Central Nervous System Axons in a Phenotypically Appropriate Manner That Correlates With Expression of L1. The Journal of Comparative Neurology 413, 495, 1999.

22. Tuszynski, M.H., Gabriel, K., Gage, F.H., Suhr, S., Meyer, S., and Rosetti, A. Nerve growth factor delivery by gene transfer induces differential outgrowth of sensory, motor, and noradrenergic neurites after adult spinal cord injury. Exp Neurol 137, 157, 1996.

23. Tuszynski, M.H., Murai, K., Blesch, A., Grill, R., and Miller, I. Functional characterization of NGF-secreting cell grafts to the acutely injured spinal cord. Cell Transplant 6, 361, 1997.

24. Jakeman, L.B., Wei, P., Guan, Z., and Stokes, B.T. Brain-derived neurotrophic factor stimulates hindlimb stepping and sprouting of cholinergic fibers after spinal cord injury. Exp Neurol 154, 170, 1998.

25. Oudega, M., and Hagg, T. Neurotrophins promote regeneration of sensory axons in the adult rat spinal cord. Brain Res 818, 431, 1999.

26. Blesch, A., Diergardt, N., and Tuszynski, M.H. Cellularly delivered GDNF induces robust growth of motor and sensory axons in the injured adult spinal cord. 1998, p. 555.

27. Schnell, L., Schneider, R., Kolbeck, R., Barde, Y.A., and Schwab, M.E. Neurotrophin-3 enhances sprouting of corticospinal tract during development and after adult spinal cord lesion. Nature 367, 170, 1994.

28. Grill, R., Murai, K., Blesch, A., Gage, F.H., and Tuszynski, M.H. Cellular delivery of neurotrophin-3 promotes corticospinal axonal growth and partial functional recovery after spinal cord injury. J Neurosci 17, 5560, 1997.

29. Weiss, P., and Taylor, A.C. Further experimental evidence against "neurotropism" in nerve regeneration. J Exp Zool 95, 233, 1944.

30. Glasby, M.A., Gschmeissner, S.E., Huang, C.L., and De Souza, B.A. Degenerated muscle grafts used for peripheral nerve repair in primates. J Hand Surg [Br] 11, 347, 1986.

31. Norris, R.W., Glasby, M.A., Gattuso, J.M., and Bowden, R.E. Peripheral nerve repair in humans using muscle autografts. A new technique. J Bone Joint Surg Br 70, 530, 1988.

32. Walton, R.L., Brown, R.E., Matory, W.E., Jr., Borah, G.L., and Dolph, J.L. Autogenous vein graft repair of digital nerve defects in the finger: a retrospective clinical study. Plast Reconstr Surg 84, 944, 1989.

33. Tang, J.B. Vein conduits with interposition of nerve tissue for peripheral nerve defects. J Reconstr Microsurg 11, 21, 1995.

34. Hall, S. Axonal regeneration through acellular muscle grafts. J Anat 190 (Pt 1), 57, 1997.

35. Hudson, T.W., Zawko, S., Deister, C., Lundy, S., Hu, C.Y., Lee, K., and Schmidt, C.E. Optimized acellular nerve graft is immunologically tolerated and supports regeneration. Tissue Eng 10, 1641, 2004.

36. Yoshii, S., Oka, M., Shima, M., Akagi, M., and Taniguchi, A. Bridging a spinal cord defect using collagen filament. Spine 28, 2346, 2003.

37. Yoshii, S., Oka, M., Shima, M., Taniguchi, A., Taki, Y., and Akagi, M. Restoration of function after spinal cord transection using a collagen bridge. J Biomed Mater Res A 70, 569, 2004.

38. Kataoka, K., Suzuki, Y., Kitada, M., Hashimoto, T., Chou, H., Bai, H., Ohta, M., Wu, S., Suzuki, K., and Ide, C. Alginate enhances elongation of early regenerating axons in spinal cord of young rats. Tissue Eng 10, 493, 2004.

39. Suzuki, Y., Kitaura, M., Wu, S., Kataoka, K., Suzuki, K., Endo, K., Nishimura, Y., and Ide, C. Electrophysiological and horseradish peroxidase-tracing studies of nerve regeneration through alginate-filled gap in adult rat spinal cord. Neurosci Lett 318, 121, 2002.

40. Nomura, H., Tator, C.H., and Shoichet, M.S. Bioengineered strategies for spinal cord repair. J Neurotrauma 23, 496, 2006.

41. Khor, E., and Lim, L.Y. Implantable applications of chitin and chitosan. Biomaterials 24, 2339, 2003.

42. Evans, G.R., Brandt, K., Katz, S., Chauvin, P., Otto, L., Bogle, M., Wang, B., Meszlenyi, R.K., Lu, L., Mikos, A.G., and Patrick, C.W., Jr. Bioactive poly(L-lactic acid) conduits seeded with Schwann cells for peripheral nerve regeneration. Biomaterials 23, 841, 2002.

43. Borgens, R.B., Shi, R., and Bohnert, D. Behavioral recovery from spinal cord injury following delayed application of polyethylene glycol. J Exp Biol 205, 1, 2002.

44. Dalton, P.D., Flynn, L., and Shoichet, M.S. Manufacture of poly(2-hydroxyethyl methacrylate-co-methyl methacrylate) hydrogel tubes for use as nerve guidance channels. Biomaterials 23, 3843, 2002.

45. Tello, F. La influencia del neurotropismo en la regeneracion de los centros nerviosos. Trab Lab Invest Biol 9, 123, 1911.

46. Smith, G.M., and Silver, J. Transplantation of immature and mature astrocytes and their effect on scar formation in the lesioned central nervous system. Prog Brain Res 78, 353, 1988.

47. Martin, D.L. Synthesis and release of neuroactive substances by glial cells. Glia 5, 81, 1992.

48. Boyd, J.G., Doucette, R., and Kawaja, M.D. Defining the role of olfactory ensheathing cells in facilitating axon remyelination following damage to the spinal cord. Faseb J 19, 694, 2005.

49. Cummings, B.J., Uchida, N., Tamaki, S.J., Salazar, D.L., Hooshmand, M., Summers, R., Gage, F.H., and Anderson, A.J. Human neural stem cells differentiate and promote locomotor recovery in spinal cord-injured mice. Proc Natl Acad Sci U S A 102, 14069, 2005.

50. Huang, D.W., McKerracher, L., Braun, P.E., and David, S. A therapeutic vaccine approach to stimulate axon regeneration in the adult mammalian spinal cord. Neuron 24, 639, 1999.

51. Sicotte, M., Tsatas, O., Jeong, S.Y., Cai, C.Q., He, Z., and David, S. Immunization with myelin or recombinant Nogo-66/MAG in alum promotes axon regeneration and sprouting after corticospinal tract lesions in the spinal cord. Mol Cell Neurosci 23, 251, 2003.

52. Benowitz, L.I., and Yin, Y. Combinatorial treatments for promoting axon regeneration in the CNS: strategies for overcoming inhibitory signals and activating neurons' intrinsic growth state. Dev Neurobiol 67, 1148, 2007.

53. Papadopoulos, C.M., Tsai, S.Y., Alsbiei, T., O'Brien, T.E., Schwab, M.E., and Kartje, G.L. Functional recovery and neuroanatomical plasticity following middle cerebral artery occlusion and IN-1 antibody treatment in the adult rat. Ann Neurol 51, 433, 2002.

54. Weidner, N., Grill, R.J., and Tuszynski, M.H. Elimination of basal lamina and the collagen "scar" after spinal cord injury fails to augment corticospinal tract regeneration. Exp Neurol 160, 40, 1999.

55. Bradbury, E.J., Moon, L.D., Popat, R.J., King, V.R., Bennett, G.S., Patel, P.N., Fawcett, J.W., and McMahon, S.B. Chondroitinase ABC promotes functional recovery after spinal cord injury. Nature 416, 636, 2002.

56. Barritt, A.W., Davies, M., Marchand, F., Hartley, R., Grist, J., Yip, P., McMahon, S.B., and Bradbury, E.J. Chondroitinase ABC promotes sprouting of intact and injured spinal systems after spinal cord injury. J Neurosci 26, 10856, 2006.

57. Puchala, E., and Windle, W.F. The possibility of structural and functional restitution after spinal cord injury. A review. Exp Neurol 55, 1, 1977.

58. Guth, L., Albuquerque, E.X., Deshpande, S.S., Barrett, C.P., Donati, E.J., and Warnick, J.E. Ineffectiveness of enzyme therapy on regeneration in the transected spinal cord of the rat. J Neurosurg 52, 73, 1980.

59. Xu, X.M., Guenard, V., Kleitman, N., and Bunge, M.B. Axonal regeneration into Schwann cell-seeded guidance channels grafted into transected adult rat spinal cord. J Comp Neurol 351, 145, 1995.

60. Xu, X.M., Chen, A., Guénard, V., Kleitman, N., and Bunge, M.B. Bridging Schwann cell transplants promote axonal regeneration from both the rostral and caudal stumps of transected adult rat spinal cord. Journal of Neurocytology 26, 1, 1997.

61. Xu, X.M., Zhang, S.X., Li, H., Aebischer, P., and Bunge, M.B. Regrowth of axons into the distal spinal cord through a Schwann-cell-seeded mini-channel implanted into hemisected adult rat spinal cord. Eur J Neurosci 11, 1723, 1999.

62. Teng, Y.D., Lavik, E.B., Qu, X., Park, K.I., Ourednik, J., Zurakowski, D., Langer, R., and Snyder, E.Y. Functional recovery following traumatic spinal cord injury mediated by a unique polymer scaffold seeded with neural stem cells. Proc Natl Acad Sci U S A 99, 3024, 2002.

63. Lee, Y.S., Lin, C.Y., Robertson, R.T., Hsiao, I., and Lin, V.W. Motor recovery and anatomical evidence of axonal regrowth in spinal cord-repaired adult rats. J Neuropathol Exp Neurol 63, 233, 2004.

64. Blits, B., Oudega, M., Boer, G.J., Bartlett Bunge, M., and Verhaagen, J. Adeno-associated viral vector-mediated neurotrophin gene transfer in the injured adult rat spinal cord improves hind-limb function. Neuroscience 118, 271, 2003.

65. Khan, Y., and Rajadhyaksha, M.S. Glial Cells: The other cells of the nervous system. Resonance 7, 8, 2002.

66. Salzer, J.L. Clustering sodium channels at the node of Ranvier: close encounters of the axon-glia kind. Neuron 18, 843, 1997.

67. Poliak, S., and Peles, E. The local differentiation of myelinated axons at nodes of Ranvier. Nat Rev Neurosci 4, 968, 2003.

68. Bunge, R.P. The role of the Schwann cell in trophic support and regeneration. Journal of Neurology 242, 19, 1994.

69. Carey, D.J., Eldridge, C.F., Cornbrooks, C.J., Timpl, R., and Bunge, R.P. Biosynthesis of type IV collagen by cultured rat Schwann cells. J Cell Biol 97, 473, 1983.

70. Cornbrooks, C.J., Carey, D.J., McDonald, J.A., Timpl, R., and Bunge, R.P. In vivo and in vitro observations on laminin production by Schwann cells. Proc Natl Acad Sci U S A 80, 3850, 1983.

71. Williams, L.R., Longo, F.M., Powell, H.C., Lundborg, G., and Varon, S. Spatial-temporal progress of peripheral nerve regeneration within a silicone chamber: parameters for a bioassay. J Comp Neurol 218, 460, 1983.

72. Hall, S.M. The Schwann cell: a reappraisal of its role in the peripheral nervous system. Neuropathol Appl Neurobiol 4, 165, 1978.

73. Fallon, J.R. Neurite guidance by non-neuronal cells in culture: preferential outgrowth of peripheral neurites on glial as compared to nonglial cell surfaces. J Neurosci 5, 3169, 1985.

74. Miller, C., Jeftinija, S., and Mallapragada, S. Micropatterned Schwann cell-seeded biodegradable polymer substrates significantly enhance neurite alignment and outgrowth. Tissue Eng 7, 705, 2001.

75. Thompson, D.M., and Buettner, H.M. Oriented Schwann Cell Monolayers for Directed Neurite Outgrowth. Annals of Biomedical Engineering 32, 1120, 2004.

76. Guenard, V., Kleitman, N., Morrissey, T.K., Bunge, R.P., and Aebischer, P. Syngeneic Schwann cells derived from adult nerves seeded in semipermeable guidance channels enhance peripheral nerve regeneration. J Neurosci 12, 3310, 1992.

77. Rodriguez, F.J., Verdu, E., Ceballos, D., and Navarro, X. Nerve guides seeded with autologous schwann cells improve nerve regeneration. Exp Neurol 161, 571, 2000.

78. Bachelin, C., Lachapelle, F., Girard, C., Moissonnier, P., Serguera-Lagache, C., Mallet, J., Fontaine, D., Chojnowski, A., Le Guern, E., Nait-Oumesmar, B., and Baron-Van Evercooren, A. Efficient myelin repair in the macaque spinal cord by autologous grafts of Schwann cells. Brain 128, 540, 2005.

79. Guest, J.D., Rao, A., Olson, L., Bunge, M.B., and Bunge, R.P. The ability of human Schwann cell grafts to promote regeneration in the transected nude rat spinal cord. Exp Neurol 148, 502, 1997.

80. Oudega, M., and Xu, X.M. Schwann cell transplantation for repair of the adult spinal cord. J Neurotrauma 23, 453, 2006.

81. Noble, M., Fok-Seang, J., and Cohen, J. Glia are a unique substrate for the in vitro growth of central nervous system neurons. J Neurosci 4, 1892, 1984.

82. Takami, T., Oudega, M., Bates, M.L., Wood, P.M., Kleitman, N., and Bunge, M.B. Schwann cell but not olfactory ensheathing glia transplants improve hindlimb locomotor performance in the moderately contused adult rat thoracic spinal cord. J Neurosci 22, 6670, 2002.

83. Chernousov, M.A., and Carey, D.J. Schwann cell extracellular matrix molecules and their receptors. Histol Histopathol 15, 593, 2000.

84. Ceballos, D., Navarro, X., Dubey, N., Wendelschafer-Crabb, G., Kennedy, W.R., and Tranquillo, R.T. Magnetically Aligned Collagen Gel Filling a Collagen Nerve Guide Improves Peripheral Nerve Regeneration. Experimental Neurology 158, 290, 1999.

85. Dubey, N., Letourneau, P.C., and Tranquillo, R.T. Guided Neurite Elongation and Schwann Cell Invasion into Magnetically Aligned Collagen in Simulated Peripheral Nerve Regeneration. Experimental Neurology 158, 338, 1999.

86. Rosner, B.I., Hang, T., and Tranquillo, R.T. Schwann cell behavior in three-dimensional collagen gels: Evidence for differential mechano-transduction and the influence of TGF-beta 1 in morphological polarization and differentiation. Experimental Neurology 195, 81, 2005.

87. BD Biosciences. BD Matrigel Basement Membrane Matrix. 2007. http://www.bdbiosciences.com/discovery_labware/products/display_product.php?keyID=230. Date last accessed: 15 Apr 2009.

88. Dubey, N., Letourneau, P.C., and Tranquillo, R.T. Neuronal contact guidance in magnetically aligned fibrin gels: efect of variation in gel mechano-structural properties. Biomaterials 22, 1065, 2001.

89. Ahmed, Z., Underwood, S., and Brown, R.A. Nerve guide material made from fibronectin: assessment of in vitro properties. Tissue Eng 9, 219, 2003.

90. Bruder, J.M., Lee, A.P., and Hoffman-Kim, D. Biomimetic materials replicating Schwann cell topography enhance neuronal adhesion and neurite alignment in vitro. J Biomater Sci Polym Ed 18, 967, 2007.

91. Tai, H.C., and Buettner, H.M. Neurite outgrowth and growth cone morphology on micropatterned surfaces. Biotechnol Prog 14, 364, 1998.

92. Voge, C.M., Kariolis, M., MacDonald, R.A., and Stegemann, J.P. Directional conductivity in SWNT-collagen-fibrin composite biomaterials through strain-induced matrix alignment. J Biomed Mater Res A 86, 269, 2008.

93. Phillips, J.B., Bunting, S.C., Hall, S.M., and Brown, R.A. Neural tissue engineering: a self-organizing collagen guidance conduit. Tissue Eng 11, 1611, 2005.

94. Mahanthappa, N.K., Anton, E.S., and Matthew, W.D. Glial Growth Factor 2, a Soluble Neuregulin, Directly Increases Schwann Cell Motility and Indirectly Promotes Neurite Outgrowth. The Journal of Neuroscience 16, 4673, 1996.

95. Houweling, D.A., Lankhorst, A.J., Gispen, W.H., Bar, P.R., and Joosten, E.A. Collagen containing neurotrophin-3 (NT-3) attracts regrowing injured corticospinal axons in the adult rat spinal cord and promotes partial functional recovery. Exp Neurol 153, 49, 1998.

96. Balgude, A.P., Yu, X., Szymanski, A., and Bellamkonda, R.V. Agarose gel stiffness determines rate of DRG neurite extension in 3D cultures. Biomaterials 22, 1077, 2001.

97. Leach, J.B., Brown, X.Q., Jacot, J.G., Dimilla, P.A., and Wong, J.Y. Neurite outgrowth and branching of PC12 cells on very soft substrates sharply decreases below a threshold of substrate rigidity. J Neural Eng 4, 26, 2007.

98. Lin, Y.W., Cheng, C.M., Leduc, P.R., and Chen, C.C. Understanding sensory nerve mechanotransduction through localized elastomeric matrix control. PLoS ONE 4, e4293, 2009.

99. Alexander, J.K., Fuss, B., and Colello, R.J. Electric field-induced astrocyte alignment directs neurite outgrowth. Neuron Glia Biology 2, 93, 2006.

100. Robinson, K.R., and Cormie, P. Electric field effects on human spinal injury: Is there a basis in the in vitro studies? Dev Neurobiol 68, 274, 2008.

101. Hurtado, A., Moon, L.D., Maquet, V., Blits, B., Jerome, R., and Oudega, M. Poly (D,L-lactic acid) macroporous guidance scaffolds seeded with Schwann cells genetically modified to secrete a bi-functional neurotrophin implanted in the completely transected adult rat thoracic spinal cord. Biomaterials 27, 430, 2006.

102. Chen, Y.S., Hsieh, C.L., Tsai, C.C., Chen, T.H., Cheng, W.C., Hu, C.L., and Yao, C.H. Peripheral nerve regeneration using silicone rubber chambers filled with collagen, laminin and fibronectin. Biomaterials 21, 1541, 2000.

103. Einheber, S., Hannocks, M.J., Metz, C.N., Rifkin, D.B., and Salzer, J.L. Transforming growth factor-beta 1 regulates axon/Schwann cell interactions. J Cell Biol 129, 443, 1995.

104. Stephens, D.J., and Allan, V.J. Light microscopy techniques for live cell imaging. Science 300, 82, 2003.

105. Cox, G., Kable, E., Jones, A., Fraser, I., Manconi, F., and Gorrell, M.D. 3-Dimensional imaging of collagen using second harmonic generation. Journal of Structural Biology 141, 53, 2003.

106. Bjornsson, C.S., Lin, G., Al-Kofahi, Y., Narayanaswamy, A., Smith, K.L., Shain, W., and Roysam, B. Associative image analysis: a method for automated quantification of 3D multi-parameter images of brain tissue. J Neurosci Methods 170, 165, 2008.

107. Pena, A.M., Boulesteix, T., Dartigalongue, T., and Schanne-Klein, M.C. Chiroptical effects in the second harmonic signal of collagens I and IV. J Am Chem Soc 127, 10314, 2005.

108. Brown, E., and McKee, T. Dynamic imaging of collagen and its modulation in tumors in vivo using second-harmonic generation. Nature Medicine 9, 796, 2003.

109. Barocas, V.H., Girton, T.S., and Tranquillo, R.T. Engineered alignment in media equivalents: magnetic prealignment and mandrel compaction. J Biomech Eng 120, 660, 1998.

110. Costa, K.D., Lee, E.J., and Holmes, J.W. Creating alignment and anisotropy in engineered heart tissue: role of boundary conditions in a model three-dimensional culture system. Tissue Eng 9, 567, 2003.

111. Yeung, T., Georges, P.C., Flanagan, L.A., Marg, B., Ortiz, M., Funaki, M., Zahir, N., Ming, W., Weaver, V., and Janmey, P.A. Effects of substrate stiffness on cell morphology, cytoskeletal structure, and adhesion. Cell Motil Cytoskeleton 60, 24, 2005.

112. Engler, A.J., Sen, S., Sweeney, H.L., and Discher, D.E. Matrix elasticity directs stem cell lineage specification. Cell 126, 677, 2006.

113. Georges, P.C., Miller, W.J., Meaney, D.F., Sawyer, E.S., and Janmey, P.A. Matrices with compliance comparable to that of brain tissue select neuronal over glial growth in mixed cortical cultures. Biophys J 90, 3012, 2006.

114. Re, F., Zanetti, A., Sironi, M., Polentarutti, N., Lanfrancone, L., Dejana, E., and Colotta, F. Inhibition of anchorage-dependent cell spreading triggers apoptosis in cultured human endothelial cells. J Cell Biol 127, 537, 1994.

115. Chen, C.S., Mrksich, M., Huang, S., Whitesides, G.M., and Ingber, D.E. Geometric control of cell life and death. Science 276, 1425, 1997.

116. Nakao, J., Shinoda, J., Nakai, Y., Murase, S., and Uyemura, K. Apoptosis regulates the number of Schwann cells at the premyelinating stage. J Neurochem 68, 1853, 1997.

117. Guyton, A.C. Basic neuroscience: anatomy & physiology. WB Saunders Company, 1991.

118. Ellis-Behnke, R. Nano Neurology and the Four P's of Central Nervous System Regeneration: Preserve, Permit, Promote, Plasticity. Medical Clinics of North America 91, 937, 2007.

119. Lee, E.J., Holmes, J.W., and Costa, K.D. Remodeling of engineered tissue anisotropy in response to altered loading conditions. Ann Biomed Eng 36, 1322, 2008.

120. Schousboe, A., Meier, E., Drejer, J., Hertz, L., and Shahar, A. A dissection and tissue culture manual of the nervous system. New York: Liss, 203–206, 1989.

121. Milner, R., Wilby, M., Nishimura, S., Boylen, K., Edwards, G., Fawcett, J., Streuli, C., Pytela, R., and ffrench-Constant, C. Division of Labor of Schwann Cell Integrins during Migration on Peripheral Nerve Extracellular Matrix Ligands. Developmental Biology 185, 215, 1997.

122. McKasson, M.J., Huang, L., and Robinson, K.R. Chick embryonic Schwann cells migrate anodally in small electrical fields. Exp Neurol 211, 585, 2008.

123. Borgens, R.B., Shi, R., Mohr, T.J., and Jaeger, C.B. Mammalian cortical astrocytes align themselves in a physiological voltage gradient. Exp Neurol 128, 41, 1994.